HyNTP: A Distributed Hybrid Algorithm for Time Synchronization

Marcello Guarro and Ricardo G. Sanfelice

***Abstract*— This paper presents a distributed hybrid algorithm that synchronizes the time and rate of a set of clocks connected over a network. Clock measurements of the nodes are given at aperiodic time instants and the controller at each node uses these measurements to achieve synchronization. Due to the continuous and impulsive nature of the clocks and the network, we introduce a hybrid system model to effectively capture the dynamics of the system and the proposed hybrid algorithm. Moreover, the hybrid algorithm allows each agent to estimate the skew of its internal clock in order to allow for synchronization to a common timer rate. We provide sufficient conditions guaranteeing synchronization of the timers, exponentially fast, with robustness. Numerical results illustrate the synchronization property induced by the proposed algorithm as well as its performance against comparable algorithms from the literature.**

I. Introduction

A. Motivation

Since the advent of asynchronous packet-based networks in communication and information technology, the topic of clock synchronization has received significant attention due to the temporal requirements of packet-based networks for the exchange of information. In recent years, as distributed packet-based networks have evolved in terms of size, complexity, and, above all, application scope, there has been a growing need for new clock synchronization schemes with tractable design conditions to meet the demands of these evolving networks.

Distributed applications such as robotic swarms, automated manufacturing, and distributed optimization rely on precise time synchronization among distributed agents for their operation; see [1]. For example, in the case of distributed control and estimation over networks, the uncertainties of packet-based network communication requires timestamping of sensor and actuator messages in order to synchronize the information to the evolution of the dynamical system being controlled or estimated. Such a scenario is impossible without the existence of a common timescale among the non-collocated agents in the system. In fact, the lack of a shared timescale among the networked agents can result in performance degradation that can destabilize the system; see [2]. Moreover, one cannot always assume that consensus on time is a given, especially when the network associated to the distributed system is subject to perturbations such as noise, delay, or jitter. Hence, it is essential that these networked systems utilize clock synchronization schemes that establish and maintain a common timescale for their algorithms.

This research has been partially supported by the National Science Foundation under Grant no. ECS-1710621, and Grant no. CNS-1544396, by the Air Force Office of Scientific Research under Grant no. FA9550-16-1-0015, Grant no. FA9550-19-1-0053, and Grant no. FA9550-19-1-0169, and by CITRIS and the Banatao Institute at the University of California.

Marcello Guarro and Ricardo G. Sanfelice are with Department of Electrical and Computer Engineering, University of California, Santa Cruz. Email: mguarro@ucsc.edu, ricardo@ucsc.edu

B. Background and Related Work

For many networked control system settings, each agent in the system is fitted with its own internal hardware clock and one or more software clocks that inherits the dynamics of the hardware clock. In an ideal scenario, the i-th agent in the system would have a clock $\tau_i \in \mathbb{R}_{\geq 0}$ such that $\tau_i(t) = t$, where t is the global or real time. However, many hardware clocks utilize quartz-crystal or MEMS oscillators, susceptible to manufacturing imperfections and environmental factors that affect oscillator frequency; see [3] and [4]. Due to the variability in oscillator frequency, one generally considers the continuous-time dynamics of the i-th hardware clock node given by

$$\dot{\tau}_i = a_i \tag{1}$$

where $a_i \in \mathbb{R}$ defines the clock's rate of change. Solving the differential equation gives the following relationship to the ideal clock or real time reference t:

$$\tau_i(t) = a_i t + \tau_i(0) \tag{2}$$

where the initial condition $\tau_i(0)$ gives the offset from t. For a network of n agents, the notion of clock synchronization can be defined as the state of the networked system such that $\tau_i = \tau_j$ for all $i, j \in \{1, 2, \ldots, n\}$, $i \neq j$.

In an ideal setting with no delay and identical clock rates (or skews), synchronization between two nodes, Node 1 and Node 2, can be achieved by the following simple reference-based algorithm. Node 1 sends its time to Node 2. Node 2 calculates its offset relative to 1. Node 2 applies the offset correction to its clock. For the case of non-identical clock skews, a pair of measurements from Node 1 would allow Node 2 to calculate its relative skew $\frac{a_1}{a_2}$ and apply a correction accordingly. In a realistic setting, however, network communication between nodes is subject to a variety of delays to which such simple reference-based algorithms are nonrobust; see [5]. Moreover, these algorithms become cumbersome in terms of network utilization and computation as the number of nodes on the network increases.

The seminal Networking Time Protocol (NTP) presented in [6] mitigates these challenges through the implementation of a centralized algorithm. In particular, the networked agents in the system synchronize to a known reference that is either injected or provided by an elected leader agent. The effects of communication delay are mitigated via assumptions on the round-trip delay that occurs in the communication of any two nodes on the network. Conversely, other centralized approaches, such as those in [7] and [8], assume the communication delay to be negligible and instead utilize least-squares minimization to estimate the errors in the offset and rates of change between the synchronizing nodes and the elected reference agent. Unfortunately, these approaches suffer robustness issues when communication with the reference node is lost or if the random delays in the transmission do not follow a normal distribution, see [3]. Moreover, algorithms like NTP were not designed for dynamic network topologies as they rely on predefined network hierarchies that define the relationships between the reference nodes and their children. Any change to the topology requires a reconstruction of the hierarchy adding considerable delay to the synchronization of the clocks.

Recently, the observed robustness issues in the centralized protocols have motivated leader-less, consensus-based approaches by leveraging the seminal results on networked consensus in [9], [10], and [11]. In particular, the works of [1], [12], [13], and, more recently, [14] employ average consensus to give asymptotic results on clock synchronization under asynchronous and asymmetric communication topology. However, due to the constraints on the communication modeling of the system the convergence results do not hold globally. Moreover, the lack of global convergence precludes any guarantees of robust asymptotic stability; see the forthcoming Remark 3.2.

The work in [15] also considers a consensus-based approach by using a controller that uses a proportional gain to compensate for the clock rates and an integrator gain acting on an auxiliary control state that compensates for the clock offsets. Though the solution in [15] provides faster convergence than the other approaches using average consensus, the algorithm assumes periodic synchronous communication of the nodes. This assumption is relaxed in [16] by considering asynchronous communication events. The authors in [17] consider a similar relaxation but also relax assumptions on the graph structure. However, in both [16] and [17] the clocks are slower to converge compared to the synchronous communication setting. Still, both synchronous and asynchronous scenarios require a large number of iterations before synchronization is achieved. Moreover, the algorithm subjects the clocks to significant nonsmooth adjustments in clock rate and offset that may prove undesirable in certain application settings or even prevent the rigorous establishment of robustness properties.

C. Contributions

The lack of performance guarantees in the aforementioned works have motivated the design of a hybrid clock synchronization algorithm with tractable design conditions. In particular, this paper introduces a distributed hybrid algorithm that exponentially synchronizes a set of clocks connected over a network via measurements given at aperiodic time instants.

Inspired by the contributions in [18], we present a distributed hybrid algorithm to synchronize the network clocks in the presence of non-ideal clock skews while capturing the continuous and impulsive dynamics of the network into a hybrid model. To achieve synchronization with a common rate of change, the algorithm also allows for local estimation of the skew of the internal clock at each agent. The use of a hybrid systems model to solve the problem under consideration allows for the application of a Lyapunov-based analysis to show stability of a desired set of interest. Using results from [19], we show that, via a suitable change of coordinates, our distributed hybrid clock synchronization algorithm guarantees synchronization of the timers, exponentially fast, with robustness.

The main contributions of this paper are given as follows:

- In Section IV, we introduce *HyNTP*, a distributed hybrid algorithm that synchronizes the clock rates and offsets to solve the problem outlined in Section III. Moreover, we present a hybrid systems model to capture the network dynamics for the case of synchronous and aperiodic communication events. In Section V, we present a reduced model of the system and a subsequent auxiliary model that is generated from an appropriately defined change of coordinates. With the auxiliary model, we present necessary and sufficient conditions for which stability of a compact set, representing synchronization, holds. Moreover, we show that the system is robust to perturbations on the communication noise, clock drift, the desired clock rate reference, and to communication delays in Section VI.
- In Section VII, we compare the merits of our algorithm to competing algorithms in the literature.

We inform the reader that some details have been omitted due to space constraints and can be found in the technical report [20]. This work is an extension of our conference paper [21], which pertains to the nominal case and has no proofs.

D. Notation

The set of natural numbers including zero, i.e., $\{0, 1, 2, \ldots\}$ is denoted by $\mathbb{N}$. The set of natural numbers is denoted as $\mathbb{N}_{>0}$, i.e., $\mathbb{N}_{>0} = \{1, 2, \ldots\}$. The set of real numbers is denoted as $\mathbb{R}$. The set of nonnegative real numbers is denoted by $\mathbb{R}_{\geq 0}$, i.e., $\mathbb{R}_{\geq 0} = [0, \infty)$. The n-dimensional Euclidean space is denoted $\mathbb{R}^n$. Given sets A and B, $F : A \rightrightarrows B$ denotes a set-valued map from A to B. For a matrix $A \in \mathbb{R}^{n\times m}$, A^T denotes the transpose of A. Given a vector $x \in \mathbb{R}^n$, $|x|$ denotes the Euclidean norm. Given a vector $x \in \mathbb{R}^n$ and a nonempty set $\Sigma \subset \mathbb{R}^n$, $|x|_\Sigma$ denotes the Euclidean point-to-set distance, i.e., $|x|_\Sigma \doteq \inf_{y\in\Sigma}|x-y|$. Given two vectors $x \in \mathbb{R}^n$ and $y \in \mathbb{R}^m$, we use the equivalent notation $(x, y) = [x^\mathsf{T} \ y^\mathsf{T}]^\mathsf{T}$. Given a matrix $A \in \mathbb{R}^{n\times m}$, $|A| := \max\{\sqrt{|\lambda|} : \lambda \in \mathrm{eig}(A^\mathsf{T}A)\}$. For two symmetric matrices $A \in \mathbb{R}^{n\times m}$ and $B \in \mathbb{R}^{n\times m}$, $A \succ B$ means that $A - B$ is positive definite; conversely, $A \prec B$ means that $A - B$ is negative definite. A vector of N ones is denoted $\mathbf{1}_N$. The matrix I_n is used to denote the identity matrix of size $n \times n$.

II. Preliminaries

A. Preliminaries on Graph Theory

Let $\mathcal{G} = (\mathcal{V}, \mathcal{E}, A)$ be a weighted directed graph (digraph) where $\mathcal{V} = \{1, 2, \ldots, n\}$ represents the set of n nodes, $\mathcal{E} \subset \mathcal{V} \times \mathcal{V}$ the set of edges, and $A \in \{0, 1\}^{n \times n}$ represents the adjacency matrix. An edge of $\mathcal{G}$ is denoted by $e_{ij} = (i, j)$. The elements of A are denoted by a_{ij}, where $a_{ij} = 1$ if $e_{ij} \in \mathcal{E}$ and $a_{ij} = 0$ otherwise. The in-degree and out-degree of a node i are defined by $d^{in}(i) = \sum_{k=1}^{n} a_{ki}$ and $d^{out}(i) = \sum_{k=1}^{n} a_{ik}$, respectively. The largest and smallest in-degree of a digraph are given by $\bar{d} = \max_{i \in \mathcal{V}} d^{in}(i)$ and $\underline{d} = \min_{i \in \mathcal{V}} d^{in}(i)$, respectively. The in-degree matrix is an $n \times n$ diagonal matrix, denoted $\mathcal{D}$, with elements given by $d_{ij} = d^{in}(i)$ if $i = j$, $d_{ij} = 0$ if $i \neq j$ for each $i \in \mathcal{V}$. The Laplacian matrix of a digraph $\mathcal{G}$, denoted by $\mathcal{L}$, is defined as $\mathcal{L} = \mathcal{D} - A$ and has the property that $\mathcal{L}\mathbf{1}_n = 0$. The set of nodes corresponding to the neighbors that share an edge with node i is denoted by $\mathcal{N}(i) := \{k \in \mathcal{V} \ : \ e_{ki} \in \mathcal{E} \}$. In the context of networks, $\mathcal{N}(i)$ represents the set of nodes for which an agent i can communicate with.

B. Preliminaries on Hybrid Systems

A hybrid system $\mathcal{H}$ in $\mathbb{R}^n$ is composed by the following *data*: a set $C \subset \mathbb{R}^n$, called the flow set; a differential equation defined by the function $f : \mathbb{R}^n \to \mathbb{R}^n$ with $C \subset \text{dom } f$, called the flow map; a set $D \subset \mathbb{R}^n$, called the jump set; and a set-valued mapping $G : \mathbb{R}^n \rightrightarrows \mathbb{R}^n$ with $D \subset \text{dom } G$, called the jump map. Then, a hybrid system $\mathcal{H} := (C, f, D, G)$ is written in the compact form

$$\mathcal{H} : \begin{cases} x \in C & \dot{x} \ = f(x) \\ x \in D & x^+ \in G(x) \end{cases} \tag{3}$$

where x is the system state. Solutions to hybrid systems are denoted by ϕ and are parameterized by (t, j), where $t \in \mathbb{R}_{\geq 0}$ defines ordinary time and $j \in \mathbb{N}$ is a counter that defines the number of jumps. A solution ϕ is defined by a *hybrid arc* on its domain dom ϕ with *hybrid time domain* structure [19]. The domain dom ϕ is a hybrid time domain if dom $\phi \subset \mathbb{R}_{\geq 0} \times \mathbb{N}$ and for each $(T, J) \in$ dom ϕ, dom $\phi \cap ([0, T] \times \{0, 1, ..., J\})$ is of the form $\bigcup_{j=0}^{J}([t_j, t_{j+1}] \times \{j\})$, with $0 = t_0 \leq t_1 \leq t_2 \leq t_{J+1}$. A function $\phi :$ dom $\phi \to \mathbb{R}^n$ is a *hybrid arc* if dom ϕ is a hybrid time domain and if for each $j \in \mathbb{N}$, the function $t \mapsto \phi(t, j)$ is locally absolutely continuous on the interval $I^j = \{t : (t, j) \in \text{dom } \phi\}$. A solution ϕ satisfies the system dynamics; see [19, Definition 2.6] for more details. A solution ϕ is said to be *maximal* if it cannot be extended by flow or a jump, and *complete* if its domain is unbounded. The set of all maximal solutions to a hybrid system $\mathcal{H}$ is denoted by $\mathcal{S}_{\mathcal{H}}$ and the set of all maximal solutions to $\mathcal{H}$ with initial condition belonging to a set A is denoted by $\mathcal{S}_{\mathcal{H}}(A)$. A hybrid system is *well-posed* if it satisfies the hybrid basic conditions in [19, Assumption 6.5].

Definition 2.1: Given a hybrid system $\mathcal{H}$ defined on $\mathbb{R}^n$, the closed set $\mathcal{A} \subset \mathbb{R}^n$ is said to be *globally exponentially stable* (GES) for $\mathcal{H}$ if there exist $\kappa, \alpha > 0$ such that every maximal solution ϕ to $\mathcal{H}$ is complete and satisfies $|\phi(t, j)|_{\mathcal{A}} \leq \kappa e^{-\alpha(t+j)} |\phi(0, 0)|_{\mathcal{A}}$ for each $(t, j) \in$ dom ϕ.

III. Problem Statement

Consider a group of n sensor nodes connected over a network represented by a digraph $\mathcal{G} = (\mathcal{V}, \mathcal{E}, A)$. Two clocks are attached to each node i of $\mathcal{G}$: an (uncontrollable) internal clock $\tau_i^* \in \mathbb{R}_{\geq 0}$ whose dynamics are given by

$$\dot{\tau}_i^* = a_i \tag{4}$$

and an adjustable clock $\tilde{\tau}_i \in \mathbb{R}_{\geq 0}$ with dynamics

$$\dot{\tilde{\tau}}_i = a_i + u_i \tag{5}$$

where $u_i \in \mathbb{R}$ is a control input. In both of these models, the (unknown) constant a_i represents the unknown drift of the internal clock.

At times t_j for $j \in \mathbb{N}_{>0}$ (we assume $t_0 = 0$), node i receives measurements $\tilde{\tau}_k$ from its neighbors, namely, for each $k \in \mathcal{N}(i)$. The resulting sequence of time instants $\{t_j\}_{j=1}^{\infty}$ is assumed to be strictly increasing and unbounded. Moreover, for such a sequence, the time elapsed between each time instant when the clock measurements are exchanged satisfies

$$T_1 \leq t_{j+1} - t_j \leq T_2, \quad 0 \leq t_1 \leq T_2 \qquad \forall j \in \mathbb{N}_{>0} \tag{6}$$

where $0 < T_1 \leq T_2$, with T_1 defining a minimum time between consecutive measurements and T_2 defines the maximum allowable transfer interval (MATI).

Remark 3.1: The models for the clocks are based on the hardware and software relationship of the real-time system that implements them. That is, the internal clock τ_i^* is treated as a type of hardware oscillator while the adjustable clock $\tilde{\tau}_i$ is treated as a virtual clock, implemented in software (as part of the proposed algorithm), that evolves according to the dynamics of the hardware oscillator. Any virtual clock implemented in node i inherits the drift parameter a_i of the internal clock, which cannot be controlled. More importantly, this drift parameter is not known due to the fact that universal time information is not available to any node. The input u_i is unconstrained as allowed by hardware platforms.

Remark 3.2: Note that the proposed communication strategy does not capture the situation when the agents in the network communicate at different times (asynchronous). The decision for modeling a synchronous communication strategy is due to the challenges in guaranteeing global, robust clock synchronization in an asynchronous setting.

For instance, in the problem settings of the work by [1], [13], and [22] the algorithms therein allow for the nodes to communicate at different time between nodes:

1) These articles consider n networked nodes whose interconnections are represented by a undirected graph $\mathcal{G}$;
2) Each node i is equipped with a local hardware clock τ_i and software clock $\hat{\tau}_i$;
3) Information is exchanged between an agent pair (i, k) at times instants $t_j^{i,k}$.

However, the convergence properties guaranteed are neither global nor robust; see [20, Remark 3.2]. In this paper, we demonstrate through the use of a simpler network model commonly used in the literature (see [15] and [17]) and the use of hybrid systems tools that such properties are possible.

Under such a setup, our goal is to design a distributed hybrid controller that, without knowledge of the drift parameter and of the communication times in advance, assigns the input u_i to drive each clock $\tilde{\tau}_i$ to synchronization with every other clock $\tilde{\tau}_k$, with $\tilde{\tau}_k$ evolving at a common prespecified constant rate of change $\sigma^* > 0$ for each $k \in \mathcal{V}$. This problem is formally stated as follows:

Problem 3.1: Given a network of n agents with dynamics as in (4) and (5) represented by a directed graph $\mathcal{G}$ and $\sigma^* > 0$, design a distributed hybrid controller that achieves the following properties when information $\tilde{\tau}_k$ for each $k \in \mathcal{N}(i)$ is received by node i at times t_j satisfying (6):

i) Global clock synchronization: for each initial condition, the components $\tilde{\tau}_1, \tilde{\tau}_2, \ldots, \tilde{\tau}_n$ of each complete solution to the system satisfy

$$\lim_{t\to\infty} |\tilde{\tau}_i(t) - \tilde{\tau}_k(t)| = 0 \qquad \forall i, k \in \mathcal{V}, i \neq k$$

ii) Common clock rate: for each initial condition, the components $\tilde{\tau}_1, \tilde{\tau}_2, \ldots, \tilde{\tau}_n$ of each complete solution to the system satisfy

$$\lim_{t\to\infty} |\dot{\tilde{\tau}}_i(t) - \sigma^*| = 0 \qquad \forall i \in \mathcal{V}$$

IV. Distributed Hybrid Controller for Time Synchronization

We define the hybrid model that provides the framework and a solution to Problem 3.1. First, since we are interested in the ability of the rate of each clock to synchronize to a constant rate σ^*, we propose the following change of coordinates: for each $i \in \mathcal{V}$, define $e_i := \tilde{\tau}_i - r$, where $r \in \mathbb{R}_{\geq 0}$ is an auxiliary variable such that $\dot{r} = \sigma^*$. The state r is only used for analysis. Then, the dynamics for e_i are given by

$$\dot{e}_i = \dot{\tilde{\tau}}_i - \sigma^* \qquad \forall i \in \mathcal{V} \tag{7}$$

By making the appropriate substitutions, one has

$$\dot{e}_i = a_i + u_i - \sigma^* \qquad \forall i \in \mathcal{V} \tag{8}$$

To model the network dynamics for aperiodic communication events at t_j's satisfying (6), we consider a timer variable τ with hybrid dynamics

$$\dot{\tau} = -1 \quad \tau \in (0, T_2], \quad \tau^+ \in [T_1, T_2] \quad \tau = 0 \tag{9}$$

This model is such that when $\tau = 0$, a communication event is triggered, and τ is reset to a point in the interval $[T_1, T_2]$ in order to preserve the bounds given in (6); see [23]. Note that τ is a global variable that models the network dynamics of the system triggering the communication events between the nodes. Moreover, information on τ is not available to the nodes. One can think of this mechanism as a type of network manager that governs the communication events of the system; see [15] and [17] for similar network models.

The proposed hybrid algorithm assigns a value to u_i so as to solve Problem 3.1, which in the e_i coordinates requires e_i to converge to zero for each $i \in \mathcal{V}$. In fact, the algorithm implements two feedback laws: a distributed feedback law and a local feedback law. The distributed feedback law utilizes a control variable $\eta_i \in \mathbb{R}$ that is impulsively updated at communication event times using both local and exchanged measurement information $\tilde{\tau}_k$. Specifically, it takes the form

$$\eta_i^+ = \sum_{k\in\mathcal{N}(i)} K_i^k(\tilde{\tau}_i, \tilde{\tau}_k)$$

where $K_i^k(\tilde{\tau}_i, \tilde{\tau}_k) := -\gamma_i(e_i - e_k)$ with $\gamma_i > 0$. Between communication event times, η_i evolves continuously.The local feedback strategy utilizes a continuous-time linear adaptive estimator with states $\hat{\tau}_i \in \mathbb{R}$ and $\hat{a}_i \in \mathbb{R}$ to estimate the drift a_i of the internal clock.[1] The estimate of the drift is then injected as feedback to compensate for the effect of a_i on the evolution of $\tilde{\tau}_i$. Furthermore, the local feedback strategy injects σ^* to attain the desired clock rate for $\tilde{\tau}_i$.

Inspired by the protocol in [18, Protocol 4.1], the dynamics of the i-th hybrid controller are given by

$$\left.\begin{aligned} \dot{u}_i &= h_i\eta_i - \mu_i(\hat{\tau}_i - \tau_i^*),\ \dot{\eta}_i = h_i\eta_i \\ \dot{\hat{a}}_i &= -\mu_i(\hat{\tau}_i - \tau_i^*),\ \dot{\hat{\tau}}_i = \hat{a}_i - (\hat{\tau}_i - \tau_i^*) \end{aligned}\right\} \ \tau \in [0, T_2]$$
$$\left.\begin{aligned} u_i^+ &= -\gamma_i \sum_{k\in\mathcal{N}(i)} (\tilde{\tau}_i - \tilde{\tau}_k) - \hat{a}_i + \sigma^*,\ \hat{a}_i^+ = \hat{a}_i \\ \eta_i^+ &= -\gamma_i \sum_{k\in\mathcal{N}(i)} (\tilde{\tau}_i - \tilde{\tau}_k),\ \hat{\tau}_i^+ = \hat{\tau}_i \end{aligned}\right\} \ \tau = 0 \tag{10}$$

where $h_i \in \mathbb{R}$, $\gamma_i > 0$ are controller parameters for the distributed hybrid consensus controller and $\mu_i > 0$ is a parameter for the local parameter estimator. The state η_i is an auxiliary controller state that is injected into the control input u_i. At communication events t_j, i.e. when $\tau = 0$, both u_i and η_i reset to new values using measurement information $\tilde{\tau}_k$ from the neighbors $k \in \mathcal{N}(i)$ of node i, as denoted by the superscript $^+$. Moreover, the values for $\hat{a}_i$ and σ^* that are injected as feedback into u_i are kept constant across jumps.

With the timer variable and hybrid controller defined in (10), we construct the hybrid closed-loop system $\mathcal{H}$ obtained from the interconnection between the distributed hybrid controller and the local adaptive estimator given in error coordinates. The state of the closed-loop system is

$$x = (e, u, \eta, \tau^*, \hat{a}, \hat{\tau}, \tau) \in \mathcal{X} \tag{11}$$

where $\mathcal{X} := \mathbb{R}^n \times \mathbb{R}^n \times \mathbb{R}^n \times \mathbb{R}^n_{\geq 0} \times \mathbb{R}^n \times \mathbb{R}^n_{\geq 0} \times [0, T_2]$ with $e = (e_1, e_2, \ldots, e_n)$, $u = (u_1, u_2, \ldots u_n)$, $\eta = (\eta_1, \eta_2, \ldots, \eta_n)$, $\tau^* = (\tau_1^*, \tau_2^*, \ldots, \tau_N^*)$, $\hat{\tau} = (\hat{\tau}_1, \hat{\tau}_2, \ldots, \hat{\tau}_N)$, $a = (a_1, a_2, \ldots, a_N)$, and $\hat{a} = (\hat{a}_1, \hat{a}_2, \ldots, \hat{a}_n)$. Then, let

$$\mathcal{H} := (C, f, D, G) \tag{12}$$

where the dynamics and data (C, f, D, G) are given by $(\dot{e}, \dot{u}, \dot{\eta}, \dot{\tau}^*, \dot{\hat{a}}, \dot{\hat{\tau}}, \dot{\tau}) = (a + u - \sigma^*\mathbf{1}_n, h\eta - \mu(\hat{\tau} - \tau^*), h\eta, a, -\mu(\hat{\tau} - \tau^*), \hat{a} - (\hat{\tau} - \tau^*), -1) =: f(x)$ for each $x \in C$ and $(e^+, u^+, \eta^+, \tau^{*+}, \hat{a}^+, \hat{\tau}^+, \tau^+) = (e, -\gamma\mathcal{L}e - \hat{a} + \sigma^*\mathbf{1}_n, -\gamma\mathcal{L}e, \tau^*, \hat{a}, \hat{\tau}, [T_1, T_2]) =: G(x)$ for each $x \in D$ where $C := \mathcal{X}$ and $D := \{x \in \mathcal{X} : \tau = 0\}$. Note that $\mathcal{X} \subset \mathbb{R}^m$ where $m = 7n$.

With the hybrid system $\mathcal{H}$ defined, the next two results establish existence of solutions to $\mathcal{H}$ and that every maximal

[1] In [20] we demonstrate the need for such a strategy to estimate a_i since first difference methods would not be viable in our problem setting.

solution to $\mathcal{H}$ is complete. In particular, we show that, through the satisfaction of some basic conditions on the hybrid system data, which is shown first, the system $\mathcal{H}$ is well-posed and that each maximal solution to the system is defined for arbitrarily large $t+j$.

Lemma 4.1: The hybrid system $\mathcal{H}$ satisfies the hybrid basic conditions defined in [19, Assumption 6.5].

Lemma 4.2: For every $\xi \in C \cup D(= \mathcal{X})$, every maximal solution ϕ to $\mathcal{H}$ with $\phi(0,0) = \xi$ is complete.

The properties given in these two lemmas are easily established from the information given in the data of $\mathcal{H}$; see [20] for full details on the proofs of these results.

With the hybrid closed-loop system $\mathcal{H}$ in (12), the set to asymptotically stabilize so as to solve Problem 3.1 is

$$\mathcal{A} := \{x \in \mathcal{X} : e_i = e_k, \eta_i = 0, \hat{a}_i = a_i, \hat{\tau}_i = \tau_i^*, \\ u_i = \eta_i - \hat{a}_i + \sigma^* \ \forall i,k \in \mathcal{V}\} \tag{13}$$

Note that $e_i = e_k$ and $\eta_i = 0$ for all $i,k \in \mathcal{V}$ imply synchronization of the clocks, meanwhile $\hat{a}_i = a_i$ and $\tau_i^* = \hat{\tau}_i$ for all $i,k \in \mathcal{V}$ ensure no error in the estimation of the clock skew and that the internal and estimated clocks are synchronized, respectively. The inclusion of $u_i = -\hat{a}_i + \sigma^*$ in $\mathcal{A}$ ensures that, for each $i \in \mathcal{V}$, e_i remains constant (at zero) so that e_i does not leave the set $\mathcal{A}$. This property is captured in the following result using the notion of forward invariance of a set.

Remark 4.3: Given that each maximal solution ϕ to $\mathcal{H}$ is complete, with the state variable τ acting as a timer for $\mathcal{H}$, for every initial condition $\phi(0,0) \in C \cup D$ we can characterize the domain of each solution ϕ to $\mathcal{H}$ as follows:

$$\text{dom } \phi = \bigcup_{j \in \mathbb{N}} [t_j, t_{j+1}] \times \{j\} \tag{14}$$

with $t_0 = 0$ and $t_{j+1} - t_j$ as in (6). Furthermore, the structure of the above hybrid time domain implies that for each $(t,j) \in$ dom ϕ we have

$$t \leq T_2(j+1) \tag{15}$$

Lemma 4.4: Given a strongly connected digraph $\mathcal{G}$, the set $\mathcal{A}$ in (13) is forward invariant for the hybrid system $\mathcal{H}$, i.e., each maximal solution ϕ to $\mathcal{H}$ with $\phi(0,0) \in \mathcal{A}$ is complete and satisfies $\phi(t,j) \in \mathcal{A}$ for each $(t,j) \in$ dom ϕ (see [19]).

With the definitions of the closed-loop system $\mathcal{H}$ in (12) and the set of interest $\mathcal{A}$ in (13) to asymptotically stabilize in order to solve Problem 3.1, we introduce our main result showing global exponential stability of $\mathcal{A}$ to $\mathcal{H}$. This result is established through an analysis of an auxiliary system $\widetilde{\mathcal{H}}_\varepsilon$ presented in (25) and its global exponential stability for the auxiliary set $\tilde{\mathcal{A}}_\varepsilon$ in (27), the details of which, along with a proofs, can be found in Section V-D.

Theorem 4.5: Given a strongly connected digraph $\mathcal{G}$, if the parameters $T_2 \geq T_1 > 0$, $\mu > 0$, $h \in \mathbb{R}$, and $\gamma > 0$, the positive definite matrices P_1, P_2, and P_3 are such that

$$P_2 A_{f_3} + A_{f_3}^\top P_2 \prec 0, \quad P_3 A_{f_4} + A_{f_4}^\top P_3 \prec 0 \tag{16}$$

$$A_{g_2}^\top \exp(A_{f_2}^\top \nu) P_1 \exp(A_{f_2}\nu) A_{g_2} - P_1 \prec 0 \quad \forall \nu \in [T_1, T_2] \tag{17}$$

$$\left| \exp\left(\frac{\bar{\kappa}_1}{\alpha_2} T_2\right)\left(1 - \frac{\bar{\kappa}_2}{\alpha_2}\right) \right| < 1 \tag{18}$$

hold, where A_{f_2}, A_{g_2} are given in (26) and

$$\begin{aligned}
&\bar{\kappa}_1 = \max\left\{\frac{\kappa_1}{2\epsilon}, \frac{\kappa_1 \epsilon}{2} - \beta_2\right\}, \quad \bar{\kappa}_2 = \min\{1, \kappa_2\} \\
&\kappa_1 = 2 \max_{\nu \in [0, T_2]} \left| \exp(A_{f_2}^\top \nu) P_1 \exp(A_{f_2}\nu) \right| \\
&\kappa_2 \in \left(0, -\min_{\nu \in [T_1, T_2]} \left\{\lambda_{min}(A_{g_2}^\top \exp(A_{f_2}^\top \nu) P_1 \exp(A_{f_2}\nu) A_{g_2} - P_1)\right\}\right) \\
&\alpha_2 = \max_{\nu \in [0, T_2]} \Big\{ \exp(2h\nu), \lambda_{max}\big(\exp(A_{f_2}^\top \nu) P_1 \exp(A_{f_2}\nu)\big), \\
&\qquad\qquad \lambda_{max}(P_2), \lambda_{max}(P_3) \Big\}
\end{aligned} \tag{19}$$

with $\epsilon > 0$, and $\beta_1 > 0$ and $\beta_2 > 0$ such that, in light of (16), $P_2 A_{f_3} + A_{f_3}^\top P_2 \preceq -\beta_1 I_2$ and $P_3 A_{f_4} + A_{f_4}^\top P_3 \preceq -\beta_2 I_{2(n-1)}$ then, the set $\mathcal{A}$ in (13) is globally exponentially stable for the hybrid system $\mathcal{H}$ in (12).

To validate our theoretical stability result in Theorem 4.5, consider five agents with dynamics as in (4) and (5) over a strongly connected digraph with the following adjacency matrix $\mathcal{G}_A = ([0,1,1,0,1], [1,0,1,0,0], [1,0,0,1,0], [0,0,1,0,1], [1,0,1,1,0])$. Given $T_1 = 0.01$, $T_2 = 0.1$, and $\sigma^* = 1$, then it can be found that the parameters $h = -1.3$, $\mu = 3$, $\gamma = 0.125$, suitable matrices P_1, P_2, P_3 (see [20] for details), and $\epsilon = 1.607$ satisfy conditions (17) and (18) in Theorem 4.5 with $\bar{\kappa}_1 = 9.78$, $\kappa_1 = 31.44$, $\bar{\kappa}_2 = 1$, and $\alpha_2 = 18.923$. Figure 1 shows the trajectories of $e_i - e_k$, ε_{a_i} for components $i \in \{1,2,3,4,5\}$ of a solution ϕ for the case where $\sigma = \sigma^*$ with initial conditions $\phi_e(0,0) = (1,-1,2,-2,0)$, $\phi_\eta(0,0) = (0,-3,1,-4,-1)$, and clock rates a_i in the range $(0.85, 1.15)$.[2]

Remark 4.6: Theorem 4.5 not only assures that the proposed algorithm guarantees global exponential stability of the set $\mathcal{A}$ defined in (13), but also that such a property is robust to perturbations — see Section VI for details. It should be noted that the property is global in all of its variables, in the sense that regardless of the initial condition for the state x of $\mathcal{H}$, in particular, convergence (in distance) to $\mathcal{A}$ is assured. These properties are not evident in other algorithms in the literature — in particular, the initial conditions for the variables τ_{new} and τ_{old} in [1, Theorem 1] need to be properly chosen to avoid unboundedness of the update law.

Remark 4.7: Observe that condition (17) may be difficult to satisfy numerically as it may not be convex in γ and P_1. The authors in [23] utilize a polytopic embedding strategy to arrive at a linear matrix inequality in which one needs to find some matrices X_i such that the exponential matrix is an element in the convex hull of the X_i matrices. Such an algorithm can be adapted to our setting.

V. Key Properties of $\mathcal{H}$ and Proof of the Main Result

A. Reduced Model – First Pass

[2]See [20] for more simulations under different scenarios including a larger simulation with $N = 100$ nodes. Code at github.com/HybridSystemsLab/HybridClockSync

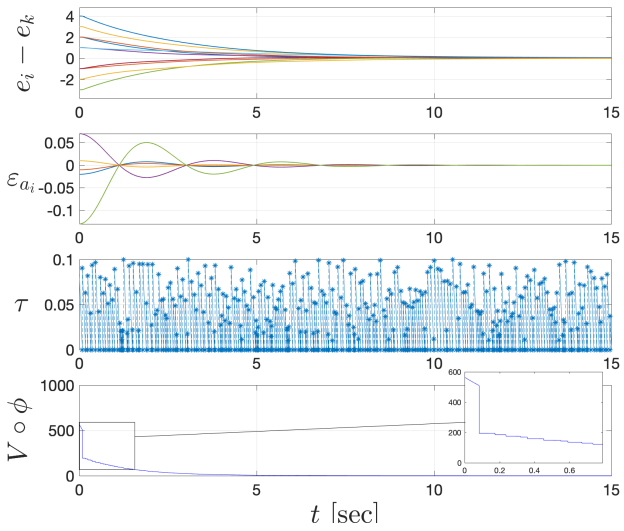

Fig. 1. The trajectories of the solution ϕ for state component errors $e_i - e_k$, ε_{a_i}, and τ. Plot of V evaluated along the solution ϕ projected onto the regular time domain (bottom).

In this section, we recast the hybrid system $\mathcal{H}$ into a reduced model obtained by setting $u = \eta - \hat{a} + \sigma^* \mathbf{1}_n$. This reduced model enables assessing asymptotic stability of $\mathcal{A}$. It is given in error coordinates for the parameter estimation of the internal clock rate and also the error of the internal clock state. We let $\varepsilon_a = a - \hat{a}$ denote the estimation error of the internal clock rate and $\varepsilon_\tau = \hat{\tau} - \tau^*$ represent the estimation error of the internal clock state. The state of the reduced model is given by $x_\varepsilon := (e, \eta, \varepsilon_a, \varepsilon_\tau, \tau) \in \mathbb{R}^n \times \mathbb{R}^n \times \mathbb{R}^n \times \mathbb{R}^n \times [0, T_2] =: \mathcal{X}_\varepsilon$ with dynamics defined by the data

$$\begin{aligned} f_\varepsilon(x_\varepsilon) &:= (\eta + \varepsilon_a, h\eta, \mu\varepsilon_\tau, -\varepsilon_\tau - \varepsilon_a, -1) \quad \forall x_\varepsilon \in C_\varepsilon, \\ G_\varepsilon(x_\varepsilon) &:= (e, -\gamma \mathcal{L} e, \varepsilon_a, \varepsilon_\tau, [T_1, T_2]) \quad \forall x_\varepsilon \in D_\varepsilon \end{aligned} \tag{20}$$

where $C_\varepsilon := \mathcal{X}_\varepsilon$ and $D_\varepsilon := \{x_\varepsilon \in \mathcal{X}_\varepsilon : \tau = 0\}$. This system is denoted $\mathcal{H}_\varepsilon = (C_\varepsilon, f_\varepsilon, D_\varepsilon, G_\varepsilon)$. Note that the construction $u = \eta - \hat{a} + \sigma^* \mathbf{1}_n$, which holds along all solutions after the first jump, leads to $\dot{e} = \eta + \varepsilon_a$.

To relate the properties of the reduced model to those of the hybrid system $\mathcal{H}$, we establish a result showing an equivalency between the solutions of $\mathcal{H}$ in (12) and $\mathcal{H}_\varepsilon$ defined above. The result shows that after the first jump, each solution ϕ to $\mathcal{H}$ is equivalent to a solution ϕ^ε to $\mathcal{H}_\varepsilon$ when the trajectories of the timer variable τ for both solutions are equal. To facilitate such a result, we define the function $M : \mathcal{X} \to \mathcal{X}_\varepsilon$ given by

$$M(x) := (e, \eta, a - \hat{a}, \hat{\tau} - \tau^*, \tau) \tag{21}$$

where $x = (e, u, \eta, \tau^*, \hat{a}, \hat{\tau}, \tau)$, as defined in (11), and the function $\widetilde{M} : \mathcal{X}_\varepsilon \times \mathbb{R}^n_{\geq 0} \times \mathbb{R}^n_{\geq 0} \to \mathcal{X}$ given by

$$\widetilde{M}(x_\varepsilon, \hat{\tau}, \tau^*) := (e, \eta - (a - \varepsilon_a) + \sigma^* \mathbf{1}_n, \eta, \hat{\tau} - \varepsilon_\tau, a - \varepsilon_a, \varepsilon_\tau + \tau^*, \tau) \tag{22}$$

Lemma 5.1: Let $T_2 \geq T_1 > 0$, digraph $\mathcal{G}$, and hybrid systems $\mathcal{H}$ and $\mathcal{H}_\varepsilon$ be given as in (12) and (20), respectively. For each $\phi \in \mathcal{S}_\mathcal{H}$ and each[3] $\phi^\varepsilon \in \mathcal{S}_{\mathcal{H}_\varepsilon}$ such that $\phi(0,0) = \widetilde{M}\big(\phi^\varepsilon(0,0), \phi_{\hat{\tau}}(0,0), \phi_{\tau^*}(0,0)\big)$ and timer components $\phi_\tau(t,j) = \phi^\varepsilon_\tau(t,j)$ for all $(t,j) \in \operatorname{dom} \phi$, it follows that $\operatorname{dom} \phi = \operatorname{dom} \phi^\varepsilon$ and $\phi(t,j) = \widetilde{M}\big(\phi^\varepsilon(t,j), \phi_{\hat{\tau}}(t,j), \phi_{\tau^*}(t,j)\big)$ for each $(t,j) \in \operatorname{dom} \phi$.

With the reduced model $\mathcal{H}_\varepsilon$ in place, we consider the following set to globally exponentially stabilize for $\mathcal{H}_\varepsilon$:

$$\mathcal{A}_\varepsilon := \{x_\varepsilon \in \mathcal{X}_\varepsilon : e_i = e_k, \eta_i = 0 \ \forall i, k \in \mathcal{V}, \varepsilon_a = 0, \varepsilon_\tau = 0\} \tag{23}$$

This set is equivalent to $\mathcal{A}$ in the sense that the point-to-set distance metrics $|x|_\mathcal{A}$ and $|x|_{\mathcal{A}_\varepsilon}$ are equivalent when the map $\widetilde{M}$ is applied, as demonstrated in the results that follow.

Lemma 5.2: Given sets $\mathcal{A}$ and $\mathcal{A}_\varepsilon$ as in (13) and (23), respectively, for each $x = (e, u, \eta, \tau^*, \hat{a}, \hat{\tau}, \tau)$, x_ε, $\hat{\tau}$, and τ^* such that $x \in \mathcal{X}$, $(x_\varepsilon, \hat{\tau}, \tau^*) \in \mathcal{X}$, and $u = \eta - \hat{a} + \sigma^* \mathbf{1}_n$ then $|x|_\mathcal{A} = |x_\varepsilon|_{\mathcal{A}_\varepsilon}$ and $|\widetilde{M}(x_\varepsilon, \hat{\tau}, \tau^*)|_\mathcal{A} = |x|_\mathcal{A}$.

Lemma 5.3: Given $T_2 \geq T_1 > 0$ and a strongly connected digraph $\mathcal{G}$, the set $\mathcal{A}$ in (13) is GES for the hybrid system $\mathcal{H}$ if $\mathcal{A}_\varepsilon$ in (23) is GES for the hybrid system $\mathcal{H}_\varepsilon$.

For proofs, see [20] and the Appendix.

B. Reduced Model – Second Pass

Global exponential stability of $\mathcal{A}_\varepsilon$ for $\mathcal{H}_\varepsilon$ is established by performing a Lyapunov analysis on a version of $\mathcal{H}_\varepsilon$ obtained after an appropriate change of coordinates, one where the flow and jump dynamics are linearized. The model is obtained by exploiting an important property of the eigenvalues of the Laplacian matrix for strongly connected digraphs.

To this end, let $\mathcal{G}$ be a strongly connected digraph. By exploiting certain known properties of strongly connected graphs as outlined in [20, Lemma 2.1] and [20, Lemma 2.2], one has that zero is a simple eigenvalue of the Laplacian matrix $\mathcal{L}$ with an associated eigenvector $v_1 = \frac{1}{\sqrt{N}} \mathbf{1}_N$. Furthermore, there exists a nonsingular matrix

$$\mathcal{T} = [v_1, \mathcal{T}_1] \tag{24}$$

where $\mathcal{T}_1 \in \mathbb{R}^{N \times N-1}$ is a matrix whose columns are the remaining eigenvectors of $\mathcal{L}$, i.e., $[v_2, \ldots, v_N]$, such that $\mathcal{T}^{-1} \mathcal{L} \mathcal{T} = \begin{bmatrix} 0 & 0 \\ 0 & \bar{\mathcal{L}} \end{bmatrix}$, where $\mathcal{L}$ is the graph Laplacian of $\mathcal{G}$ and $\bar{\mathcal{L}}$ is a diagonal matrix with the nonnegative eigenvalues of $\mathcal{L}$ as the diagonal elements given by $(\lambda_2, \lambda_3, \ldots, \lambda_N)$, see [9], [10], and [24] for more details.

To perform the said change of coordinates, we use $\mathcal{T}$ to first perform the following transformations: $\bar{e} = \mathcal{T}^{-1} e$, $\bar{\eta} = \mathcal{T}^{-1} \eta$, $\bar{\varepsilon}_a = \mathcal{T}^{-1} \varepsilon_a$ and $\bar{\varepsilon}_\tau = \mathcal{T}^{-1} \varepsilon_\tau$. Then, we define vectors $\bar{z} = (\bar{z}_1, \bar{z}_2)$ and $\bar{w} = (\bar{w}_1, \bar{w}_2)$, where $\bar{z}_1 := (\bar{e}_1, \bar{\eta}_1)$, $\bar{z}_2 := (\bar{e}_2, \ldots, \bar{e}_N, \bar{\eta}_2, \ldots, \bar{\eta}_N)$, $\bar{w}_1 = (\bar{\varepsilon}_{a_1}, \bar{\varepsilon}_{\tau_1})$, and $\bar{w}_2 = (\bar{\varepsilon}_{a_2}, \ldots, \bar{\varepsilon}_{a_n}, \bar{\varepsilon}_{\tau_2}, \ldots, \bar{\varepsilon}_{\tau_n})$. Finally, we define $\chi_\varepsilon := (\bar{z}_1, \bar{z}_2, \bar{w}_1, \bar{w}_2, \tau) \in \mathbb{R}^2 \times \mathbb{R}^{2(n-1)} \times \mathbb{R}^2 \times \mathbb{R}^{2(n-1)} \times [0, T_2] =: \mathcal{X}_\varepsilon$ as the state of the new version of $\mathcal{H}_\varepsilon$, which is denoted

[3]Note that for a given solution $\phi^\varepsilon(t,j)$ to $\mathcal{H}_\varepsilon$, the solution components are given by $\phi^\varepsilon(t,j) = \big(\phi^\varepsilon_e(t,j), \phi^\varepsilon_\eta(t,j), \phi^\varepsilon_{\varepsilon_a}(t,j), \phi^\varepsilon_{\varepsilon_\tau}(t,j), \phi^\varepsilon_\tau(t,j)\big)$.

$\widetilde{\mathcal{H}}_\varepsilon$ and has data given by

$$\widetilde{f}_\varepsilon(\chi_\varepsilon):=\begin{bmatrix}A_{f_1}\bar{z}_1\\ A_{f_2}\bar{z}_2\\ A_{f_3}\bar{w}_1\\ A_{f_4}\bar{w}_2\\ -1\end{bmatrix}+\begin{bmatrix}B_{f_1}\bar{w}_1\\ B_{f_2}\bar{w}_2\\ 0\\ 0\\ 0\end{bmatrix},\ \widetilde{G}_\varepsilon(\chi_\varepsilon):=\begin{bmatrix}A_{g_1}\bar{z}_1\\ A_{g_2}\bar{z}_2\\ \bar{w}_1\\ \bar{w}_2\\ [T_1,T_2]\end{bmatrix} \tag{25}$$

for each χ_ε in $\widetilde{C}_\varepsilon := \mathcal{X}_\varepsilon$ and in $\widetilde{D}_\varepsilon := \{\chi_\varepsilon \in \mathcal{X}_\varepsilon : \tau = 0\}$, respectively, with

$$\begin{aligned}&A_{f_1}=\begin{bmatrix}0 & 1\\ 0 & h\end{bmatrix}, && A_{f_2}=\begin{bmatrix}0 & I_m\\ 0 & hI_m\end{bmatrix}, && A_{f_3}=\begin{bmatrix}0 & \mu\\ -1 & -1\end{bmatrix}\\ &A_{f_4}=\begin{bmatrix}0 & \mu I_m\\ -I_m & -I_m\end{bmatrix}, && B_{f_1}=\begin{bmatrix}1 & 0\\ 0 & 0\end{bmatrix}, && B_{f_2}=\begin{bmatrix}I_m & 0\\ 0 & 0\end{bmatrix}\\ &A_{g_1}=\begin{bmatrix}1 & 0\\ 0 & 0\end{bmatrix}, && A_{g_2}=\begin{bmatrix}I_m & 0\\ -\gamma\bar{\mathcal{L}} & 0\end{bmatrix}\end{aligned} \tag{26}$$

and $m = N-1$. Then, $\widetilde{\mathcal{H}}_\varepsilon = (\widetilde{C}_\varepsilon, \widetilde{f}_\varepsilon, \widetilde{D}_\varepsilon, \widetilde{G}_\varepsilon)$ denotes the new version of $\mathcal{H}_\varepsilon$. The set $\mathcal{A}_\varepsilon$ to stabilize in the new coordinates for this hybrid system is given by

$$\widetilde{\mathcal{A}}_\varepsilon := \{\chi_\varepsilon \in \mathcal{X}_\varepsilon : \bar{z}_1{=}(e^*, 0), \bar{z}_2{=}0, \bar{w}_1{=}0, \bar{w}_2{=}0, e^*{\in}\mathbb{R}\} \tag{27}$$

In the following two results, we first demonstrate the relationship between the sets $\tilde{\mathcal{A}}_\varepsilon$ for $\widetilde{\mathcal{H}}_\varepsilon$ and $\mathcal{A}_\varepsilon$ for $\mathcal{H}_\varepsilon$ so as to solve Problem 3.1. Then, similar to Lemma 5.3, we show that global exponential stability of $\tilde{\mathcal{A}}_\varepsilon$ for $\widetilde{\mathcal{H}}_\varepsilon$ implies global exponential stability of $\mathcal{A}_\varepsilon$ for $\mathcal{H}_\varepsilon$. See the appendix for proofs.

Lemma 5.4: Let $T_2 \geq T_1 > 0$, digraph $\mathcal{G}$, and hybrid systems $\mathcal{H}_\varepsilon$ and $\widetilde{\mathcal{H}}_\varepsilon$ be given as in (20) and (25), respectively. For each solution $\phi \in \mathcal{S}_{\mathcal{H}_\varepsilon}$ there exists a solution $\tilde{\phi} \in \mathcal{S}_{\widetilde{\mathcal{H}}_\varepsilon}$ such that $\phi(t,j) = \Gamma\tilde{\phi}(t,j)$ for each $(t,j) \in$ dom ϕ if and only if for each solutions $\tilde{\phi} \in \mathcal{S}_{\widetilde{\mathcal{H}}_\varepsilon}$ there exists a solution $\phi \in \mathcal{S}_{\mathcal{H}_\varepsilon}$ such that $\tilde{\phi}(t,j) = \Gamma^{-1}\phi(t,j)$ for each $(t,j) \in$ dom $\tilde{\phi}$, where $\Gamma = \text{diag}(\mathcal{T}, \mathcal{T}, \mathcal{T}, \mathcal{T}, 1)$.

Lemma 5.5: Given $0 < T_1 \leq T_2$ and a strongly connected digraph $\mathcal{G}$, $\xi \in \mathcal{A}_\varepsilon$ if and only if $\chi_\varepsilon := \Gamma^{-1}\xi \in \tilde{\mathcal{A}}_\varepsilon$, where $\Gamma^{-1} = \text{diag}(\mathcal{T}^{-1}, \mathcal{T}^{-1}, \mathcal{T}^{-1}, \mathcal{T}^{-1}, 1)$ and $\mathcal{T}$ is given in (24). Moreover, for each $x_\varepsilon \in \mathcal{X}_\varepsilon$ and each $\chi_\varepsilon \in \mathcal{X}_\varepsilon$, $|\chi_\varepsilon|_{\tilde{\mathcal{A}}_\varepsilon} \leq |\Gamma^{-1}||x_\varepsilon|_{\mathcal{A}_\varepsilon}$ and $|x_\varepsilon|_{\mathcal{A}_\varepsilon} \leq |\Gamma||\chi_\varepsilon|_{\tilde{\mathcal{A}}_\varepsilon}$.

Lemma 5.6: Given $0 < T_1 \leq T_2$ and a strongly connected digraph $\mathcal{G}$, the set $\tilde{\mathcal{A}}_\varepsilon$ is GES for the hybrid system $\widetilde{\mathcal{H}}_\varepsilon$ if and only if $\mathcal{A}_\varepsilon$ is GES for the hybrid system $\mathcal{H}_\varepsilon$.

C. Parameter Estimator

Exponential stability of the set $\tilde{\mathcal{A}}_\varepsilon$ for $\widetilde{\mathcal{H}}_\varepsilon$ hinges upon the convergence of the estimate $\hat{a}$ to a. We present a result establishing convergence of $\hat{a}$ to a by considering a model reduction of $\widetilde{\mathcal{H}}_\varepsilon$. To this end, consider the state $\chi_{\varepsilon_r} := (\bar{w}_1, \bar{w}_2, \tau) \in \mathbb{R}^2 \times \mathbb{R}^{2(n-1)} \times [0, T_2] =: \mathcal{X}_{\varepsilon_r}$. Its dynamics are given by the system $\widetilde{\mathcal{H}}_{\varepsilon_r} = (\widetilde{C}_{\varepsilon_r}, \widetilde{f}_{\varepsilon_r}, \widetilde{D}_{\varepsilon_r}, \widetilde{G}_{\varepsilon_r})$ with data $\widetilde{f}_\varepsilon(\chi_{\varepsilon_r})$ for each $\chi_{\varepsilon_r} \in \widetilde{C}_{\varepsilon_r}$ and $\widetilde{G}_{\varepsilon_r}(\chi_{\varepsilon_r})$ for each $\chi_{\varepsilon_r} \in \widetilde{D}_{\varepsilon_r}$ where

$$\begin{aligned}\widetilde{f}_{\varepsilon_r}(\chi_{\varepsilon_r}) &:= \big(A_{f_3}\bar{w}_1, A_{f_4}\bar{w}_2, -1\big),\\ \widetilde{G}_{\varepsilon_r}(\chi_{\varepsilon_r}) &:= \big(\bar{w}_1, \bar{w}_2, [T_1, T_2]\big)\end{aligned} \tag{28}$$

where $\widetilde{C}_{\varepsilon_r} := \mathcal{X}_{\varepsilon_r}$ and $\widetilde{D}_{\varepsilon_r} := \{\chi_{\varepsilon_r}{\in}\mathcal{X}_{\varepsilon_r} : \tau = 0\}$. For this system, the set to exponentially stabilize is given by

$$\widetilde{\mathcal{A}}_{\varepsilon_r} := \{0\} \times \{0\} \times [0, T_2] \tag{29}$$

In the next result, we show global exponential stability of the set $\tilde{\mathcal{A}}_{\varepsilon_r}$ for $\widetilde{\mathcal{H}}_{\varepsilon_r}$ through the satisfaction of matrix inequalities. See the appendix for proof.

Proposition 5.7: If there exists a positive scalar μ and positive definite symmetric matrices P_2, P_3 such that, with A_{f_3} and A_{f_4} as in (26), the conditions in (16) hold, then the set $\tilde{\mathcal{A}}_{\varepsilon_r}$ is globally exponentially stable for the hybrid system $\widetilde{\mathcal{H}}_{\varepsilon_r}$. Furthermore, every solution $\tilde{\phi}$ to $\widetilde{\mathcal{H}}_{\varepsilon_r}$ satisfies

$$|\tilde{\phi}(t,j)|_{\tilde{\mathcal{A}}_{\varepsilon_r}} \leq \sqrt{\frac{\alpha_{\bar{w}_2}}{\alpha_{\bar{w}_1}}}\exp\Big(-\frac{\bar{\gamma}\tilde{\beta}}{2\alpha_{\bar{w}_2}}(t+j)\Big)|\tilde{\phi}(0,0)|_{\tilde{\mathcal{A}}_{\varepsilon_r}} \tag{30}$$

for each $(t,j) \in$ dom $\tilde{\phi}$, with $\alpha_{\bar{w}_1} = \min\{\lambda_{min}(P_2), \lambda_{min}(P_3)\}$, $\alpha_{\bar{w}_2} = \max\{\lambda_{max}(P_2), \lambda_{max}(P_3)\}$, $\tilde{\beta} > 0$, and $\bar{\gamma} = \min\{1-\gamma, \gamma T_1\}$.

D. Proof of Theorem 4.5

Consider the following Lyapunov function candidate for $\widetilde{\mathcal{H}}_\varepsilon$

$$V(\chi_\varepsilon) := V_1(\chi_\varepsilon) + V_2(\chi_\varepsilon) + V_{\varepsilon_r}(\chi_\varepsilon) \quad \forall \chi_\varepsilon \in \mathcal{X}_\varepsilon \tag{31}$$

where $V_1(\chi_\varepsilon){=}\exp(2h\tau)\bar{\eta}_1^2$,

$$V_2(\chi_\varepsilon){=}\bar{z}_2^\top \exp(A_{f_2}^\top\tau)P_1\exp(A_{f_2}\tau)\bar{z}_2$$

and $V_{\varepsilon_r}(\chi_\varepsilon) = \bar{w}_1^\top P_2\bar{w}_1 + \bar{w}_2^\top P_3\bar{w}_2$. Note that there exist two positive scalars α_1, α_2 such that

$$\alpha_1|\chi_\varepsilon|^2_{\tilde{\mathcal{A}}_\varepsilon} \leq V(\chi_\varepsilon) \leq \alpha_2|\chi_\varepsilon|^2_{\tilde{\mathcal{A}}_\varepsilon} \quad \forall \chi_\varepsilon \in \tilde{C}_\varepsilon \cup \tilde{D}_\varepsilon \tag{32}$$

With P_1 positive definite and noting the nonsingularity of $\exp(A_{f_2}\tau)$ for every τ, we have $\alpha_1 = \min\limits_{\nu\in[0,T_2]}\Big\{\exp(2h\nu), \lambda_{min}\big(\exp(A_{f_2}^\top\nu)P_1\exp(A_{f_2}\nu)\big), \lambda_{min}(P_2), \lambda_{min}(P_3)\Big\}$ and α_2 as in (19). For each $\chi_\varepsilon \in \tilde{C}_\varepsilon$, one has

$$\begin{aligned}\langle\nabla V(\chi_\varepsilon), \tilde{f}_\varepsilon(\chi_\varepsilon)\rangle = 2\bar{z}_2^\top\big(\exp(A_{f_2}^\top\tau)P_1\exp(A_{f_2}\tau)\big)B_{f_2}\bar{w}_2\\ + \bar{w}_1^\top(P_2A_{f_3} + A_{f_3}^\top P_2)\bar{w}_1\\ + \bar{w}_2^\top(P_3A_{f_4} + A_{f_4}^\top P_3)\bar{w}_2\end{aligned} \tag{33}$$

Now, by noting the conditions in (16), with $\beta_1 > 0$ and $\beta_2 > 0$ such that $P_2A_{f_3} + A_{f_3}^\top P_2 \leq -\beta_1 I$, and $P_3A_{f_4} + A_{f_4}^\top P_3 \leq -\beta_2 I$ then one has

$$\langle\nabla V(\chi_\varepsilon), \tilde{f}_\varepsilon(\chi_\varepsilon)\rangle \leq \kappa_1|\bar{z}_2||\bar{w}_2| - \beta_1|\bar{w}_1|^2 - \beta_2|\bar{w}_2|^2 \tag{34}$$

where κ_1 is as given in (19). Applying Young's inequality to $\kappa_1|\bar{z}_2||\bar{w}_2|$,[4] we obtain

$$\langle\nabla V(\chi_\varepsilon), \tilde{f}_\varepsilon(\chi_\varepsilon)\rangle \leq \frac{\kappa_1}{2\epsilon}|\bar{z}_2|^2 - \beta_1|\bar{w}_1|^2 + \Big(\frac{\kappa_1\epsilon}{2} - \beta_2\Big)|\bar{w}_2|^2 \tag{35}$$

where $\epsilon > 0$. We then upper bound the inequality by picking the largest coefficient, i.e, $\bar{\kappa}_1 = \max\Big\{\frac{\kappa_1}{2\epsilon}, \Big(\frac{\kappa_1\epsilon}{2} - \beta_2\Big)\Big\}$, leading to

$$\langle\nabla V(\chi_\varepsilon), \tilde{f}_\varepsilon(\chi_\varepsilon)\rangle \leq \frac{\bar{\kappa}_1}{\alpha_2}V(\chi_\varepsilon) \tag{36}$$

[4] In particular, we are utilizing the relation $ab \leq \frac{a^2}{2\epsilon} + \frac{\epsilon b^2}{2}$ where $a, b \in \mathbb{R}$ and $\epsilon > 0$.

Now, for the analysis across jumps, note that for all $\chi_\varepsilon \in \tilde{D}_\varepsilon$, $\tau = 0$. At jumps, τ is mapped to some point $\nu \in [T_1, T_2]$. Then, at jumps, for each $g \in \tilde{G}_\varepsilon$ one has

$$\begin{aligned} V(g)-V(\chi_\varepsilon) = \\ -\bar{\eta}_1^2+\bar{z}_2^\top \big(A_{g_2}^\top \exp\left(A_{f_2}^\top \nu\right) P_1 \exp\left(A_{f_2}\nu\right) A_{g_2} - P_1\big)\bar{z}_2 \\ \leq -\bar{\kappa}_2\big(|\bar{\eta}_1|^2 + |\bar{z}_2|^2\big) \end{aligned}$$

where $\bar{\kappa}_2$ and κ_2 are as given in (19), from where we have

$$V(g) - V(\chi_\varepsilon) \leq -\bar{\kappa}_2\big(|\bar{\eta}_1|^2 + |\bar{z}_2|^2\big) \tag{37}$$

Utilizing the upper bound α_2 from the definition of V in (32), for all $\chi_\varepsilon \in \tilde{D}_\varepsilon$, one has $V(\chi_\varepsilon) \leq \alpha_2\big(|\bar{\eta}_1|^2 + |\bar{z}_2|^2 + |\bar{w}|^2\big)$. Dividing by α_2 and rearranging terms, one has

$$-(|\bar{\eta}_1|^2 + |\bar{z}_2|^2) \leq -\frac{1}{\alpha_2}V(\chi_\varepsilon) + |\bar{w}|^2 \tag{38}$$

Then, by inserting (38) into (37), we obtain

$$V(g) - V(\chi_\varepsilon) \leq \bar{\kappa}_2\Big(-\frac{1}{\alpha_2}V(\chi_\varepsilon) + |\bar{w}|^2\Big) \tag{39}$$

Now, by noting that $\langle \nabla V(\chi_\varepsilon), \tilde{f}(\chi_\varepsilon)\rangle \leq \frac{\bar{\kappa}_1}{\alpha_2}V(\chi_\varepsilon)$ and by (39), pick a solution $\tilde{\phi}$ to $\widetilde{\mathcal{H}}_\varepsilon$ with initial condition $\tilde{\phi}(0,0) \in \widetilde{C}_\varepsilon \cup \widetilde{D}_\varepsilon$. Let the jumps of $\tilde{\phi}$ occur at times $(t_j, j) \in \{j' : \exists t' : (t', j') \in \text{dom } \phi\}$. For each $(t, j) \in [0, t_1] \times \{0\}$ one has

$$V(\tilde{\phi}(t,0)) \leq \exp\Big(\frac{\bar{\kappa}_1}{\alpha_2}t_1\Big)V(\tilde{\phi}(0,0))$$

At $(t_1, 1)$, one has

$$V(\tilde{\phi}(t_1,1)) \leq \Big(1-\frac{\bar{\kappa}_2}{\alpha_2}\Big)\exp\Big(\frac{\bar{\kappa}_1}{\alpha_2}t_1\Big)V(\tilde{\phi}(0,0)) + \bar{\kappa}_2|\bar{w}(t_1,0)|^2$$

Then, for each $(t, j) \in [t_1, t_2] \times \{1\}$

$$\begin{aligned} V(\tilde{\phi}(t,1)) = \exp\Big(\frac{\bar{\kappa}_1}{\alpha_2}t_2\Big)\Big(1-\frac{\bar{\kappa}_2}{\alpha_2}\Big)V(\tilde{\phi}(0,0)) \\ + \exp\big(\frac{\bar{\kappa}_1}{\alpha_2}(t_2-t_1)\big)\bar{\kappa}_2|\bar{w}(t_1,0)|^2 \end{aligned}$$

At $(t_2, 2)$, one has

$$\begin{aligned} V(\tilde{\phi}(t_2,2)) \leq \exp\Big(\frac{\bar{\kappa}_1}{\alpha_2}t_2\Big)\Big(1-\frac{\bar{\kappa}_2}{\alpha_2}\Big)^2 V(\tilde{\phi}(0,0)) \\ + \bar{\kappa}_2\Big[\exp\Big(\frac{\bar{\kappa}_1}{\alpha_2}(t_2-t_1)\Big)|\bar{w}(t_1,0)|^2 + |\bar{w}(t_2,1)|^2\Big] \end{aligned}$$

A general form of the bound is given by

$$\begin{aligned} V(\tilde{\phi}(t,j)) \leq \exp\Big(\frac{\bar{\kappa}_1}{\alpha_2}t_j\Big)\Big(1-\frac{\bar{\kappa}_2}{\tilde{\alpha}_1}\Big)^j V(\tilde{\phi}(0,0)) \\ + \bar{\kappa}_2\Big(\sum_{k=1}^{j}\exp\Big(\frac{\bar{\kappa}_1}{\alpha_2}(t_{k+1}-t_k)\Big)|\bar{w}(t_k,k-1)|^2\Big) \end{aligned} \tag{40}$$

Noting that $t_{j+1} - t_j \leq T_2$ and $\frac{\bar{\kappa}_1}{\alpha_2} > 0$, the latter term can be further bounded as

$$\begin{aligned} \bar{\kappa}_2\Big(\sum_{k=1}^{j}\exp\big(\frac{\bar{\kappa}_1}{\alpha_2}(t_{k+1}-t_k)\big)|\bar{w}(t_k,k-1)|^2\Big) \\ \leq \bar{\kappa}_2\exp\big(\frac{\bar{\kappa}_1}{\alpha_2}T_2\big)\sup_{(t,j)\in\text{dom}\tilde{\phi}}|\bar{w}(t,j)|^2 \end{aligned}$$

Moreover, since $t_j \leq T_2(j+1)$ and $\frac{\bar{\kappa}_1}{\alpha_2} > 0$, we can also put a stricter bound on the first term in (40) as follows:

$$\begin{aligned} \exp\Big(\frac{\bar{\kappa}_1}{\alpha_2}t_j\Big)\Big(1-\frac{\bar{\kappa}_2}{\alpha_2}\Big)^j V(\tilde{\phi}(0,0)) \\ \leq \exp\Big(\frac{\bar{\kappa}_1}{\alpha_2}T_2\Big)\Big(\exp\Big(\frac{\bar{\kappa}_1}{\alpha_2}T_2\Big)\Big(1-\frac{\bar{\kappa}_2}{\alpha_2}\Big)\Big)^j V(\tilde{\phi}(0,0)) \end{aligned}$$

Thus

$$\begin{aligned} V(\tilde{\phi}(t,j)) \leq \\ \exp\Big(\frac{\bar{\kappa}_1}{\alpha_2}T_2\Big)\Big(\exp\Big(\frac{\bar{\kappa}_1}{\alpha_2}T_2\Big)\Big(1-\frac{\bar{\kappa}_2}{\alpha_2}\Big)\Big)^j V(\tilde{\phi}(0,0)) \\ + \bar{\kappa}_2\exp\Big(\frac{\bar{\kappa}_1}{\alpha_2}T_2\Big)\sup_{(t,j)\in\text{dom}\tilde{\phi}}|\bar{w}(t,j)|^2 \end{aligned}$$

Then, from the result of Proposition 5.7, we have (30) with $\alpha_{\bar{w}_1} = \min\{\lambda_{min}(P_2), \lambda_{min}(P_3)\}$ and $\alpha_{\bar{w}_2} = \max\{\lambda_{max}(P_2), \lambda_{max}(P_3)\}$. Now, to improve readability, we have omitted including the use of the notation $V(\tilde{\phi}(t,j))$ when evaluating V along the trajectory for the solution $\tilde{\phi}$ opting instead for the use of the state components of χ_ε directly. In particular, we remind the reader that the notation $\bar{w}(t,j)$ corresponds to the $\bar{w}$ component of a solution, i.e., $\phi_{\bar{w}}(t,j)$. Now, combining the inequality with (32) and noting $V(\tilde{\phi}(0,0)) \leq \alpha_2|\tilde{\phi}(0,0)|^2_{\tilde{\mathcal{A}}_\varepsilon}$ one has for each $(t,j) \in \text{dom } \phi$

$$\begin{aligned} |\phi(t,j)|_{\tilde{\mathcal{A}}_\varepsilon} \leq \\ \sqrt{\frac{\alpha_2}{\alpha_1}}|\phi(0,0)|_{\tilde{\mathcal{A}}_\varepsilon}\exp\Big(\frac{\bar{\kappa}_1}{2\alpha_2}T_2\Big)\Big(\exp\Big(\frac{\bar{\kappa}_1}{2\alpha_2}T_2\Big)\Big(1-\frac{\bar{\kappa}_2}{2\alpha_2}\Big)\Big)^j \\ +\sqrt{\bar{\kappa}_2}\exp\Big(\frac{\bar{\kappa}_1}{2\alpha_2}T_2\Big)\sqrt{\frac{\alpha_{\bar{w}_2}}{\alpha_{\bar{w}_1}}\exp\Big(\frac{-\bar{\gamma}\tilde{\beta}}{2\alpha_{\bar{w}_2}}(t+j)\Big)^2|\phi_{\bar{w}}(0,0)|^2_{\tilde{\mathcal{A}}_{\varepsilon r}}} \end{aligned} \tag{41}$$

By the given conditions, the set $\tilde{\mathcal{A}}_\varepsilon$ is globally exponentially stable and attractive for $\widetilde{\mathcal{H}}_\varepsilon$. Now, by utilizing Lemmas 5.4 - 5.6, we can establish global exponential stability to the set $\mathcal{A}_\varepsilon$ for $\mathcal{H}_{\bar{\varepsilon}}$. In particular, Lemma 5.4 establishes the relation between $\widetilde{\mathcal{H}}_\varepsilon$ and $\mathcal{H}_\varepsilon$. In turn, we can then make use of Lemmas 5.1 - 5.3, where Lemma 5.1 establishes the reduction from $\mathcal{H}$ to $\mathcal{H}_\varepsilon$, to show that the set $\mathcal{A}$ is globally exponentially stable and attractive for $\mathcal{H}$ in (12).

VI. Robustness to Communication Noise, Clock Drift Perturbations, and Error on σ

Under a realistic scenario, it is often the case that the system is subjected to disturbances. In this section, we present results on input-to-state stability (ISS) of the system when it is affected by different types of disturbances. First, we present an ISS result that considers communication noise. Then, we present an ISS result on the parameter estimation sub-system when it is subjected to noise on the internal clock output. Finally, we present an ISS result on noise introduced to the desired clock rate reference σ^*.

Definition 6.1: (Input-to-state stability) A hybrid system $\mathcal{H}$ with input m is input-to-state stable with respect to a set $\mathcal{A} \subset \mathbb{R}^n$ if there exist $\beta \in \mathcal{KL}$ and $\kappa \in \mathcal{K}$ such that each solution pair (ϕ, m) to $\mathcal{H}$ satisfies $|\phi(t,j)|_{\mathcal{A}} \leq \max\{\beta(|\phi(0,0)|_{\mathcal{A}}, t+j), \kappa(|m|_\infty)\}$ for each $(t,j) \in \text{dom } \phi$.

A. Robustness to Communication Noise

We consider the case when the measurements of the timer $\tilde{\tau}_i$ is affected by noise $m_{e_i} \in \mathbb{R}$, $i \in \mathcal{V}$. As a result, the output of each agent is given by $\tilde{\tau}_i + m_{e_i}$. In the presence of this noise, the update law to η_i^+ in the hybrid controller in (10) becomes

$$\eta_i^+ = -\gamma \sum_{k\in\mathcal{N}(i)} (\tilde{\tau}_i - \tilde{\tau}_k) - \gamma \sum_{k\in\mathcal{N}(i)} (m_{e_i} - m_{e_k})$$

Performing the same change of coordinates, as in the proof of Theorem 4.5, we show that $\widetilde{\mathcal{H}}_\varepsilon$ is ISS to communication noise $m_e := (m_{e_1}, m_{e_2}, \ldots, m_{e_n}) \in \mathbb{R}^n$. Recalling the change of coordinates $\bar{e} = \mathcal{T}^{-1}e$ and $\bar{\eta} = \mathcal{T}^{-1}\eta$, let $\bar{m}_e = \mathcal{T}^{-1}m_e$. The update law $\bar{\eta}^+$, is given by $\bar{\eta}^+ = (0, -\gamma\bar{\mathcal{L}}\bar{e} - \gamma\bar{\mathcal{L}}\bar{m}_e)$ with $\bar{\eta}_1$ unaffected by the communication noise.

Using the update law for $\bar{\eta}$ under the effect of $\bar{m}_e$, we define the perturbed hybrid system $\widetilde{\mathcal{H}}_m$ with state vector $\chi_m := (\bar{z}_1, \bar{z}_2, \bar{w}_1, \bar{w}_2, \tau) \in \mathcal{X}_\varepsilon$, where, again $\bar{z}_1 = (\bar{e}_1, \bar{\eta}_1)$, $\bar{z}_2 = (\bar{e}_2, \ldots, \bar{e}_N, \bar{\eta}_2, \ldots, \bar{\eta}_N)$, $\bar{w}_1 = (\bar{\varepsilon}_{a_1}, \bar{\varepsilon}_{\tau_1})$, and $\bar{w}_2 = (\bar{\varepsilon}_{a_2}, \ldots, \bar{\varepsilon}_{a_n}, \bar{\varepsilon}_{\tau_2}, \ldots, \bar{\varepsilon}_{\tau_n})$. Moreover, let $\bar{m}_{\bar{z}_2} = (0, \bar{m}_e)$. The data $(\widetilde{C}_m, \tilde{f}_m, \widetilde{D}_m, \widetilde{G}_m)$ for the new system $\widetilde{\mathcal{H}}_m$ is given by $\tilde{f}_m(\chi_m) := \tilde{f}_\varepsilon(\chi_m)$ for each $\chi_m \in \widetilde{C}_m$ and $\widetilde{G}_m(\chi_m, \bar{m}_\varepsilon) := \widetilde{G}_\varepsilon(\chi_m) - (0, B_g\bar{m}_{\bar{z}_2}, 0, 0, 0)$ for each $\chi_m \in \widetilde{D}_m$ where $\widetilde{C}_m := \mathcal{X}_\varepsilon$, $\widetilde{D}_m := \{\chi_m \in \mathcal{X}_m : \tau = 0\}$, and $B_g = \begin{bmatrix} 0 & \gamma\bar{\mathcal{L}} \end{bmatrix}^\top$.

Theorem 6.2: Given a strongly connected digraph $\mathcal{G}$, if the parameters $T_2 \geq T_1 > 0$, $\mu > 0$, $h \in \mathbb{R}$, $\gamma > 0$, and positive definite symmetric matrices P_1, P_2, and P_3 are such that (17) and (18) hold, the hybrid system $\mathcal{H}_m$ with input $\bar{m}_e$ is ISS with respect to $\widetilde{\mathcal{A}}_\varepsilon$ in (27). Furthermore, for each $(t, j) \in$ dom ϕ every solution ϕ to $\widetilde{\mathcal{H}}_m$ satisfies $|\phi(t,j)|_{\widetilde{\mathcal{A}}_\varepsilon} \leq$

$$\sqrt{\frac{\alpha_2}{\alpha_1}}|\phi(0,0)|_{\widetilde{\mathcal{A}}_\varepsilon} \exp\left(\frac{\bar{\kappa}_1}{2\alpha_2}T_2\right)\left(\exp\left(\frac{\bar{\kappa}_1}{2\alpha_2}T_2\right)\left(1-\frac{\bar{\kappa}_2}{2\alpha_2}\right)\right)^j$$
$$+\sqrt{\bar{\kappa}_2}\exp\left(\frac{\bar{\kappa}_1}{2\alpha_2}T_2\right)\sqrt{\frac{\alpha_{\bar{w}_2}}{\alpha_{\bar{w}_1}}}\exp\left(\frac{-\bar{\gamma}\tilde{\beta}}{2\alpha_{\bar{w}_2}}(t+j)\right)^2|\phi_{\bar{w}}(0,0)|^2_{\widetilde{\mathcal{A}}_{\varepsilon_r}}$$
$$+\sqrt{\bar{\kappa}_{\bar{m}_2}}\exp\left(\frac{\kappa}{4\epsilon_2}T_2\right)\sqrt{\sup_{(t,j)\in\text{dom }\phi}|\bar{m}_{\bar{z}_2}(t,j)|^2}$$

The proof of this result utilizes a Lyapunov analysis using the function candidate V in (31). Since the disturbance is present during jumps, we show that V can be upper bounded resulting in a bounded disturbance in V when evaluated along a given solution to $\widetilde{\mathcal{H}}_{m_\sigma}$; see [20] for more details.

B. Robustness to Perturbations on Internal Clock Drift

In this section, we consider a disturbance $m_{\tau_i^*} \in \mathbb{R}$, $i \in \mathcal{V}$ added to the output of the internal clock. Let $y_i^{\tau^*} := \tau_i^* + m_{\tau_i^*}$, $i \in \mathcal{V}$, define the perturbed internal clock output. Then the dynamics of the original estimation system in (12) under this disturbance becomes

$$\begin{aligned} &\dot{\hat{\tau}}_i = \hat{a}_i - (\hat{\tau}_i - y_i^{\tau^*}), \quad \dot{\hat{a}}_i = -\mu(\hat{\tau}_i - y_i^{\tau^*}) && \tau \in [0, T_2] \\ &\hat{\tau}_i^+ = \hat{\tau}_i, \qquad\qquad\quad \hat{a}_i^+ = \hat{a}_i && \tau = 0 \end{aligned} \tag{42}$$

In error coordinates $\varepsilon_{\hat{a}_i} = a_i - \hat{a}_i$, $\varepsilon_{\tau_i} = \hat{\tau}_i - \tau_i^*$, this leads to

$$\begin{aligned} &\dot{\varepsilon}_{\tau_i} = -\varepsilon_{\tau_i} - \varepsilon_{a_i} + m_{\tau_i^*}, \; \dot{\varepsilon}_{\hat{a}_i} = \mu\varepsilon_{\tau_i} - \mu m_{\tau_i^*} && \tau \in [0, T_2] \\ &\varepsilon_{\tau_i}^+ = \varepsilon_{\tau_i}, \qquad\qquad\quad \varepsilon_{a_i}^+ = \varepsilon_{a_i} && \tau = 0 \end{aligned}$$

Similar to the result presented in Proposition 5.7, for the estimation sub-system we will consider the same reduction $\widetilde{\mathcal{H}}_{\varepsilon_r}$ that now captures the perturbation. Recall the coordinate transformations $\bar{\varepsilon}_a = \mathcal{T}^{-1}\varepsilon_a$ and $\bar{\varepsilon}_\tau = \mathcal{T}^{-1}\varepsilon_\tau$ for the respective internal clock and parameter estimation errors. Moreover, recall $\bar{w} = (\bar{w}_1, \bar{w}_2)$ where $\bar{w}_1 = (\bar{\varepsilon}_{a_1}, \bar{\varepsilon}_{\tau_1})$ and $\bar{w}_2 = (\bar{\varepsilon}_{a_2}, \ldots, \bar{\varepsilon}_{a_n}, \bar{\varepsilon}_{\tau_2}, \ldots, \bar{\varepsilon}_{\tau_n})$. Let $\bar{m}_{\tau^*} = \mathcal{T}^{-1}m_{\tau^*}$ and $\bar{q} = (\bar{q}_1, \bar{q}_2)$ where $\bar{q}_1 = (\bar{m}_{\tau_1^*}, \bar{m}_{\tau_1^*})$ and $\bar{q}_2 = (\bar{m}_{\tau_2^*}, \ldots, \bar{m}_{\tau_n^*}, \bar{m}_{\tau_2^*}, \ldots, \bar{m}_{\tau_n^*})$. Now, consider the reduced coordinates $\chi_{m_r} := (\bar{w}_1, \bar{w}_2, \tau) \in \mathbb{R}^n \times \mathbb{R}^n \times [0, T_2] =: \mathcal{X}_\varepsilon$. The data of this reduced system is given by $\widetilde{\mathcal{H}}_{m_r} = (\widetilde{C}_\varepsilon, \widetilde{f}_\varepsilon, \widetilde{D}_\varepsilon, \widetilde{G}_\varepsilon)$ where $\widetilde{f}_{m_r}(\chi_{m_r}, \bar{q}) := \widetilde{f}_{\varepsilon_r}(\chi_{m_r}) + (B_{m_1}\bar{q}_1, B_{m_2}\bar{q}_2, 0)$ for each $\chi_{m_r} \in \widetilde{C}_{m_r}$ and $\widetilde{G}_{m_r}(\chi_{m_r}) := (\bar{w}_1, \bar{w}_2, [T_1, T_2])$ for each $\chi_{m_r} \in \widetilde{D}_{m_r}$ where $\widetilde{C}_{m_r} := \mathcal{X}_\varepsilon$, $\widetilde{D}_{m_r} := \{\chi_m \in \mathcal{X}_\varepsilon : \tau = 0\}$, and $B_{m_1} = ([\mu, 0], [0, 1])$, $B_{m_2} = ([\mu I, 0], [0, I])$.

Theorem 6.3: If there exists a positive scalar μ and positive definite symmetric matrices P_2, P_3 such that the conditions in (16) hold, the hybrid system $\mathcal{H}_{mr}$ with input $\bar{m}_{\tau^*}$ is ISS with respect to $\widetilde{\mathcal{A}}_{\varepsilon_r}$ given in (29).

The proof of this result is established by picking a solution to the model reduction $\widetilde{\mathcal{H}}_{\varepsilon_r}$, integrating the disturbance that is treated as an input to the system, and then bounding the integral. A proof of this result can be found in [20].

C. Robustness to Error on σ

In this section, we consider a disturbance on σ^* to capture the scenario where σ^* is not precisely known, i.e., $\sigma_i \neq \sigma^*$. Let $\varepsilon_{\sigma_i} = \sigma_i - \sigma^*$ represent the error between the injected and the ideal clock rate. Treating ε_σ as a perturbation to the system $\mathcal{H}_\varepsilon$, one has $\dot{x}_\varepsilon = f_\varepsilon(x_\varepsilon) + (\varepsilon_\sigma, 0, 0, 0, 0)$ for each $x_\varepsilon \in C_\varepsilon$ and $x_\varepsilon^+ \in (e, -\gamma\mathcal{L}e, \varepsilon_a, \varepsilon_\tau, [T_1, T_2])$ for each $x_\varepsilon \in D_\varepsilon$. To show how the perturbation affects $\widetilde{\mathcal{H}}_\varepsilon$, let $\bar{\varepsilon}_\sigma = \mathcal{T}^{-1}\varepsilon_\sigma$, then let $\bar{m}_\sigma = (\bar{m}_{\sigma_1}, \bar{m}_{\sigma_2})$ where $\bar{m}_{\sigma_1} = \bar{\varepsilon}_{\sigma_1}$ and $\bar{m}_{\sigma_2} = (\bar{\varepsilon}_{\sigma_2}, \ldots, \bar{\varepsilon}_{\sigma_n})$.

We define this perturbed hybrid system $\widetilde{\mathcal{H}}_{m_\sigma}$ with state vector $\chi_{m_\sigma} := (\bar{z}_1, \bar{z}_2, \bar{w}_1, \bar{w}_2, \tau) \in \mathcal{X}_\varepsilon$. Its dynamics are given by the new system $\widetilde{\mathcal{H}}_{m_\sigma} = (\tilde{C}_{m_\sigma}, \tilde{f}_{m_\sigma}, \tilde{D}_{m_\sigma}, \tilde{G}_{m_\sigma})$ with data $\tilde{f}_{m_\sigma}(\chi_{m_\sigma})$ for each $\chi_{m_\sigma} \in \tilde{C}_{m_\sigma} := \mathcal{X}_\varepsilon$ and $\tilde{G}_{m_\sigma}(\chi_{m_\sigma})$ for each $\chi_{m_\sigma} \in \tilde{D}_{m_\sigma} := \{\chi_{m_\sigma} \in \mathcal{X}_\varepsilon : \tau = 0\}$ where $\tilde{f}_{m_\sigma}(\chi_{m_\sigma}, \bar{m}_\sigma) := \tilde{f}_\varepsilon(\chi_{m_\sigma}) + (\bar{m}_{\sigma_1}, \bar{m}_{\sigma_2}, 0, 0, 0)$ and $\widetilde{G}_{m_\sigma}(\chi_{m_\sigma}) := \widetilde{G}_\varepsilon(\chi_{m_\sigma})$ leading to the following result.

Theorem 6.4: Given a strongly connected digraph $\mathcal{G}$, if the parameters $T_2 \geq T_1 > 0$, $\mu > 0$, $h \in \mathbb{R}$, $\gamma > 0$, and positive definite symmetric matrices P_1, P_2, and P_3 are such that (17) and (18) hold, the hybrid system $\widetilde{\mathcal{H}}_{m_\sigma}$ with input $\bar{m}_\sigma$ is ISS with respect to $\widetilde{\mathcal{A}}_\varepsilon$ given in (27).

The proof of this result largely follows the same approach used in the proof of Theorem 6.2, namely, a Lyapunov analysis using the function candidate V in (31). Since the disturbance is present during flows, we show that the derivative of V can be upper bounded resulting in a bounded disturbance in V when evaluated along a given solution to $\widetilde{\mathcal{H}}_{m_\sigma}$; see [20] for more details.

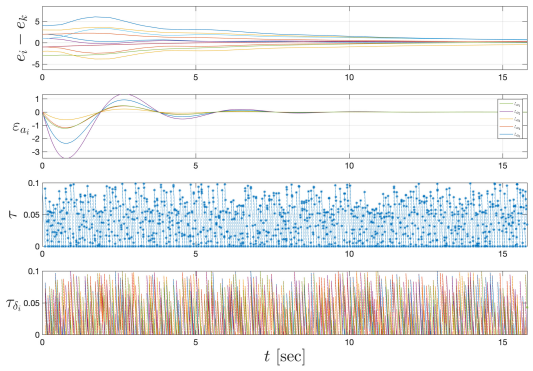

Fig. 2. The trajectories of the solution ϕ for state component errors $e_i - e_k$, ε_{a_i}, τ, and τ_{δ_i}

D. Robustness to Communication Event Delays

In this section, we consider communication delays and show that the asymptotic stability of $\mathcal{H}$ is robust (in a practical sense) to them. To model communication delays, we define a new hybrid system, denoted $\mathcal{H}_\delta$, that is an augmentation of $\widetilde{\mathcal{H}}_\varepsilon$ implementing the following mechanism: when a communication event is triggered due to τ reaching zero, the information to communicate is stored in a memory state and only available to the agents after T^δ seconds after. Due to space constraints, the details behind the construction of $\mathcal{H}_\delta$ are in [20].

Theorem 6.5: Given a strongly connected digraph $\mathcal{G}$, if the parameters $T_2 \geq T_1 > 0$, $\mu > 0$, $h \in \mathbb{R}$, $\gamma > 0$, and the positive definite symmetric matrices P_1, P_2, and P_3 are such that the conditions in Theorem 4.5 hold, then the set $\mathcal{A}$ is semiglobally practically asymptotically stability with respect to T^δ for $\mathcal{H}$ in (12), namely, for each compact set $K \subset \mathcal{X}$ and each $\epsilon > 0$, there exist a class $\mathcal{KL}$-function β and $T^\delta > 0$ such that each solution ϕ_{x_δ} to $\mathcal{H}$ with $\phi_{x_\delta}(0,0) \in K$ and with communication delay no larger than T^δ satisfies $|\phi_{x_\delta}(t,j)|_{\mathcal{A}} \leq \beta(|\phi_{x_\delta}(0,0)|_{\mathcal{A}}, t+j) + \varepsilon$ for all $(t,j) \in \operatorname{dom} \phi_{x_\delta}$.

The proof of this result follows from [25, Theorem 5.3] using the notions given in [25, Section VII-C]. Complete details and a proof of Theorem 6.5 can be found in [20], along with a numerical validation. To emphasize the robustness of $\mathcal{H}$ to small delays, Figure 2 depicts trajectories to a decentralized delay scenario where the data from each node incurs a maximum delay of $T^\delta = 0.1$ seconds, modeled by a delay timer τ_{δ_i} for each node.

VII. Comparisons

In this section, we compare our algorithm to several consensus-based clock synchronization algorithms from the literature through a numerical example. We consider a four agent setting and simulate each algorithm presented in [15] (PI-Consensus), [17] (RandSync), and [1] (Average TimeSync) to our hybrid algorithm HyNTP as in (12).

Consider $N = 4$ agents with clock dynamics as in (4) and (5) over a strongly connected graph with the following adjacency matrix $\mathcal{G}_A = [0,1,0,1]$, $[1,0,1,0]$, $[0,1,0,1]$, $[1,0,1,0]$ and aperiodic communication events such that successive communications events are lower and upper bounded

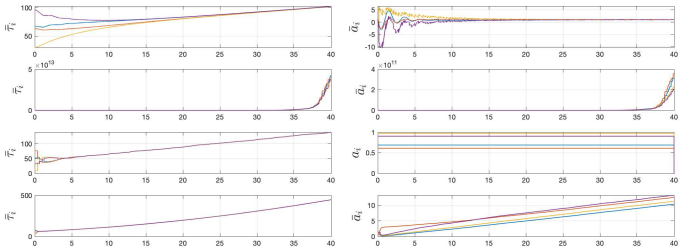

(a) (b)

Fig. 3. The evolution of the trajectories of the adjustable clocks $\bar{\tau}_i$ (3a) and adjustable clock rates $\bar{a}_i$ (3b) for each clock synchronization algorithm. From top to bottom, *HyNTP*, *Average TimeSync*, *PI-Consensus*, and *RandSync*.

by $T_1 = 0.1$ and $T_2 = 0.5$, respectively. The initial conditions for the clock rates $\bar{a}_i$ and adjustable clock values $\bar{\tau}_i$ for each $i \in \mathcal{V}$ has been randomly chosen within the intervals $(0.5, 1.5)$ and $(0, 200)$, respectively. Moreover, consider the case where the system is subjected to a communication noise $m_{\tau_i}(t,j) \in (0,1)$ on the clock measurements. Figure 3a and 3b show the trajectories of $\bar{\tau}$ and $\bar{a}_i$, respectively, for agents $i \in \{1,2,3,4\}$ for the *HyNTP* algorithm and each of the comparison algorithms under consideration.

For the *HyNTP* algorithm, setting $\sigma^* = 1$, it can be found that the parameters $h = -2$, $\mu = 9$, $\gamma = 0.06$ and $\epsilon = 4.752$ with suitable matrices P_1, P_2, and P_3 satisfy conditions (17) and (18) in Theorem 4.5 with $\bar{\kappa}_1 = 2.02$, $\kappa_1 = 19.22$, $\bar{\kappa}_2 = 1$, and $\alpha_2 = 44.03$.

VIII. Conclusion

In this paper, we modeled a network of clocks with aperiodic communication that utilizes a distributed hybrid controller to achieve synchronization, using the hybrid systems framework. Results were given to guarantee and show synchronization of the timers, exponentially fast. Numerical results validating the exponentially fast convergence of the timers were also given. Numerical results were also provided to demonstrate performance against a similar class of clock synchronization algorithms.

Appendix

Proof of Lemma 4.4: Pick an initial condition $\xi \in \mathcal{A}$. Let ϕ be a maximal solution to $\mathcal{H}$ with $\phi(0,0) = \xi$.[5]

- Consider the case where $\phi(0,0) \in \mathcal{A} \setminus D$. The initial conditions of the components of ϕ satisfy $\phi_{e_i}(0,0) = \phi_{\eta_i}(0,0) = 0$ for the clock errors e_i, $\phi_{\hat{\tau}_i}(0,0) = \phi_{\tau_i^*}(0,0)$ for the estimated clocks $\hat{\tau}_i$, $\phi_{\hat{a}_i}(0,0) = \phi_{a_i}(0,0)$ for the clock rates $\hat{a}_i$ and $\phi_{u_i}(0,0) = \phi_{\eta_i}(0,0) - \phi_{\hat{a}_i}(0,0) + \sigma^*$ for the control input for each $i \in \mathcal{V}$. With f being linear affine, the constrained differential equation $\dot{x} = f(x)$ $x \in C$ has unique solutions. Let $[0,t_1] \times \{0\} \subset \operatorname{dom} \phi$ with $t_1 > 0$, which exists since $\phi(0,0) \in \mathcal{A} \setminus D$. From the definition of f, the solution components of the states u, η, and e during this interval

[5]Note that for a given solution $\phi(t,j)$ to $\mathcal{H}$, the solution components are given by $\phi(t,j) = (\phi_e(t,j), \phi_u(t,j), \phi_\eta(t,j), \phi_{\tau^*}(t,j), \phi_{\hat{a}}(t,j), \phi_{\hat{\tau}}(t,j), \phi_\tau(t,j))$

remain constant. From the definition of f in (12) we have that the components of the solution ϕ satisfy $\phi_{e_i}(t,j) = \phi_{e_k}(t,j)$, $\phi_\eta(t,j) = 0$, $\phi_{\hat{a}_i}(t,j) = \phi_{a_i}(t,j)$, $\phi_{\hat{\tau}_i}(t,j) = \phi_{\tau_i^*}(t,j)$, and $\phi_{u_i}(t,j) = \phi_{\eta_i}(t,j) - \phi_{\hat{a}_i}(t,j) + \sigma^*$ for each $(t,j) \in [0,t_1]\times\{0\}$. Therefore, the solution ϕ does not leave the set $\mathcal{A}$ when $\phi(0,0) \in \mathcal{A}\setminus D$.

- Consider the case where $\phi(0,0) \in \mathcal{A}\cap D$. Since flow is not possible from $\phi(0,0)$ as $\phi_\tau(0,0) = 0$, $(\{0\}\times\{0\}) \cup (\{0\}\times\{1\}) \subset \text{dom }\phi$ as the solution ϕ jumps initially. By inspection, the jump map G in (12) only affects the states η, u, and τ, with the other state components unchanged. Since the quantity $-\gamma\mathcal{L}e$ in the jump map is zero at $\phi(0,0)$, we have that $\phi_\eta(0,1) = -\gamma\mathcal{L}\phi_e(0,0) = 0$. Moreover, since $\hat{a}$ is constant across jumps, $\phi_{\hat{a}}(0,1) = \phi_{\hat{a}}(0,0)$, then, $\phi_u(0,1) = -\gamma\mathcal{L}\phi_e(0,0) - \phi_{\hat{a}}(0,0) + \sigma^*\mathbf{1}_n$ $\phi_\eta(0,1) - \phi_{\hat{a}}(0,1) + \sigma^*\mathbf{1}_n$ The timer τ resets to a point in the interval $[T_1,T_2]$, namely, $\phi_\tau(0,1) \in [T_1,T_2]$. Then, the full solution ϕ at $(0,1)$ satisfies $\phi(0,1) \in \mathcal{A}$.

Since these properties hold for each $\xi \in \mathcal{A}$, $\mathcal{A}$ is forward invariant for $\mathcal{H}$. ■

Proof of Lemma 5.2: For each $x \in \mathcal{X}$, the distance from x to the set $\mathcal{A}$ is given as $|x|_\mathcal{A} = \inf_{y\in\mathcal{A}}|x-y|$. Evaluating the distance directly, one has $|x|_\mathcal{A} = \inf_{e^*\in E}\text{sqrt}\big((e-e^*)^\top(e-e^*) + (u-\eta+\hat{a}-\sigma^*\mathbf{1}_n)^\top(u-\eta+\hat{a}-\sigma^*\mathbf{1}_n) + \eta^\top\eta + (\hat{a}-a)^\top(\hat{a}-a) + (\hat{\tau}-\tau^*)^\top(\hat{\tau}-\tau^*)\big)$ where $E := \{e^* \in \mathbb{R}^n : e_i^* = e_k^* \ \forall i,k \in \mathcal{V}\}$. When $u = \eta - \hat{a} + \sigma^*\mathbf{1}_n$ we have $|x|_\mathcal{A} = \inf_{e^*\in E}\text{sqrt}\big((e-e^*)^\top(e-e^*) + \eta^\top\eta + (\hat{a}-a)^\top(\hat{a}-a) + (\hat{\tau}-\tau^*)^\top(\hat{\tau}-\tau^*)\big)$. For each $x_\varepsilon \in \mathcal{X}_\varepsilon$, the distance from x_ε to the set $\mathcal{A}_\varepsilon$ is given as $|x_\varepsilon|_{\mathcal{A}_\varepsilon} = \inf_{y\in\mathcal{A}_\varepsilon}|x_\varepsilon - y|$. Evaluating the distance directly, one has $|x_\varepsilon|_{\mathcal{A}_\varepsilon} = \inf_{e^*\in E}\text{sqrt}\big((e-e^*)^\top(e-e^*) + \eta^\top\eta + \varepsilon_a^\top\varepsilon_a + \varepsilon_\tau^\top\varepsilon_\tau\big)$. Making the appropriate substitutions for ε_τ and ε_a, we get $|x_\varepsilon|_{\mathcal{A}_\varepsilon} = \inf_{e^*\in E}\text{sqrt}\big((e-e^*)^\top(e-e^*) + \eta^\top\eta + (\hat{a}-a)^\top(\hat{a}-a) + (\hat{\tau}-\tau^*)^\top(\hat{\tau}-\tau^*)\big)$. Now, for each $(x_\varepsilon,\hat{\tau},\tau^*) \in \mathcal{X}$, the distance from the point $\widetilde{M}(x_\varepsilon,\hat{\tau},\tau^*)$ to the set $\mathcal{A}$ is given by $|\widetilde{M}(x_\varepsilon,\hat{\tau},\tau^*)|_\mathcal{A} = \inf_{y\in\mathcal{A}}|\widetilde{M}(x_\varepsilon,\hat{\tau},\tau^*) - y|$. Computing this distance, one has $|\widetilde{M}(x_\varepsilon,\hat{\tau},\tau^*)|_\mathcal{A} = \inf_{e^*\in E,\alpha_{\tau^*}\in\mathbb{R}^n_{\geq 0},\alpha_\tau\in[0,T_2]}|(e,\eta-(a-\varepsilon_a)+\sigma^*\mathbf{1}_n,\eta,\ \hat{\tau}-\varepsilon_\tau, a-\varepsilon_a,\varepsilon_\tau+\tau^*,\tau) - (e^*,\eta-\hat{a}+\sigma^*\mathbf{1}_n,0,\alpha_{\tau^*},a,\tau^*,\alpha_\tau)|$. Making the appropriate substitutions for ε_τ and ε_a, we get $|\widetilde{M}(x_\varepsilon,\hat{\tau},\tau^*)|_\mathcal{A} = \inf_{e^*\in E}\text{sqrt}\big((e-e^*)^\top(e-e^*) + \eta^\top\eta + (\hat{a}-a)^\top(\hat{a}-a) + (\hat{\tau}-\tau^*)^\top(\hat{\tau}-\tau^*)\big)$ Thus, we have that $|\widetilde{M}(x_\varepsilon,\hat{\tau},\tau^*)|_\mathcal{A} = |x|_\mathcal{A} = |x_\varepsilon|_{\mathcal{A}_\varepsilon}$. ■

Proof of Lemma 5.3: Suppose the set $\mathcal{A}_\varepsilon$ is GES for $\mathcal{H}_\varepsilon$. By Definition 2.1 there exist $\kappa,\alpha > 0$ such that each maximal solution ϕ^ε to $\mathcal{H}_\varepsilon$ satisfies $|\phi^\varepsilon(t,j)|_{\mathcal{A}_\varepsilon} \leq \kappa\exp(-\alpha(t+j))|\phi^\varepsilon(0,0)|_{\mathcal{A}_\varepsilon}$ for each $(t,j) \in \text{dom }\phi^\varepsilon$. Now, pick any maximal solution ϕ to $\mathcal{H}$. Through an application of Lemma 5.1, there exists a corresponding solution ϕ^ε to $\mathcal{H}_\varepsilon$ such that $\phi(t,j) = \widetilde{M}\big(\phi^\varepsilon(t,j),\phi_{\hat{\tau}}(t,j),\phi_{\tau^*}(t,j)\big)$ for each $(t,j) \in \text{dom }\phi$. Given that ϕ^ε satisfies the given exponential bound, using the relationship between distances in Lemma 5.2 we have that ϕ satisfies $|\phi(t,j)|_\mathcal{A} \leq \kappa\exp(-\alpha(t+j))|\phi(0,0)|_\mathcal{A}$. Then, the set $\mathcal{A}$ is GES for $\mathcal{H}$. ■

Proof of Lemma 5.4: Pick a solution $\tilde{\phi} \in \mathcal{S}_{\widetilde{\mathcal{H}}_\varepsilon}$. with $\tilde{\phi} = (\tilde{\phi}_{\bar{z}_1},\tilde{\phi}_{\bar{z}_2},\tilde{\phi}_{\bar{w}_1},\tilde{\phi}_{\bar{w}_2},\tau)$, however, recall that $\bar{z}_1 := (\bar{e}_1,\bar{\eta}_1)$, $\bar{z}_2 := (\bar{e}_2,\ldots,\bar{e}_N,\bar{\eta}_2,\ldots,\bar{\eta}_N)$, $\bar{w}_1 = (\bar{\varepsilon}_{a_1},\bar{\varepsilon}_{\tau_1})$, and $\bar{w}_2 = (\bar{\varepsilon}_{a_2},\ldots,\bar{\varepsilon}_{a_n},\bar{\varepsilon}_{\tau_2},\ldots,\bar{\varepsilon}_{\tau_n})$ thus, through a re-ordering of the solution trajectories, one has that with some of the above notation, $\tilde{\phi}$ can be rewritten as $\tilde{\phi} = (\tilde{\phi}_{\bar{e}},\tilde{\phi}_{\bar{\eta}},\tilde{\phi}_{\bar{\varepsilon}_a},\tilde{\phi}_{\bar{\varepsilon}_\tau},\tau)$. Then, recall the change of coordinates $\bar{e} = \mathcal{T}^{-1}e$, $\bar{\eta} = \mathcal{T}^{-1}\eta$, $\bar{\varepsilon}_a = \mathcal{T}^{-1}\varepsilon_a$, and $\bar{\varepsilon}_\tau = \mathcal{T}^{-1}\varepsilon_\tau$. Since $\mathcal{T}^{-1}$ is an invertible time-invariant linear operator, applying its inverse $\mathcal{T}$ to the components of $\tilde{\phi}$, one has $\big(\mathcal{T}\tilde{\phi}_{\bar{e}}(t,j),\mathcal{T}\tilde{\phi}_{\bar{\eta}}(t,j),\mathcal{T}\tilde{\phi}_{\bar{\varepsilon}_a}(t,j),\mathcal{T}\tilde{\phi}_{\bar{\varepsilon}_\tau}(t,j)\big) = \big(\phi_e(t,j),\phi_\eta(t,j),\phi_{\varepsilon_a}(t,j),\phi_{\varepsilon_\tau}(t,j)\big)$ for each $(t,j) \in \text{dom }\tilde{\phi}$. Noting that τ is equivalent for $\mathcal{H}_\varepsilon$ and $\widetilde{\mathcal{H}}_\varepsilon$. Therefore, it follows that$\tilde{\phi}(t,j) = \Gamma^{-1}\phi(t,j)$ for each $(t,j) \in \text{dom }\tilde{\phi}$.

Conversely, pick a solution $\phi \in \mathcal{S}_{\mathcal{H}_\varepsilon}$, let $\phi = (\phi_e,\phi_\eta,\phi_{\varepsilon_a},\phi_{\varepsilon_\tau},\tau)$ and recall the change of coordinates $\bar{e} = \mathcal{T}^{-1}e$, $\bar{\eta} = \mathcal{T}^{-1}\eta$, $\bar{\varepsilon}_a = \mathcal{T}^{-1}\varepsilon_a$, and $\bar{\varepsilon}_\tau = \mathcal{T}^{-1}\varepsilon_\tau$. Since $\mathcal{T}^{-1}$ is a time-invariant linear operator, applying it to the components of ϕ, one has $\big(\mathcal{T}^{-1}\phi_e(t,j),\mathcal{T}^{-1}\phi_\eta(t,j),\mathcal{T}^{-1}\phi_{\varepsilon_a}(t,j),\mathcal{T}^{-1}\phi_{\varepsilon_\tau}(t,j)\big) = \big(\tilde{\phi}_{\bar{e}}(t,j),\tilde{\phi}_{\bar{\eta}}(t,j),\tilde{\phi}_{\bar{\varepsilon}_a}(t,j),\tilde{\phi}_{\bar{\varepsilon}_\tau}(t,j)\big)$ for each $(t,j) \in \text{dom }\phi$. Thus, it follows that $\phi(t,j) = \Gamma\tilde{\phi}(t,j)$ for each $(t,j) \in \text{dom }\phi$. ■

Proof of Lemma 5.5: This proof has been omitted as it is simply exploits the property of norms for linear systems.

Proof of Proposition 5.6: The proof of this result has been omitted as it follows similarly to that of Lemma 5.3.

Proof of Proposition 5.7: Consider the following Lyapunov function candidate $V_{\varepsilon_r}(\chi_{\varepsilon_r}) = \bar{w}_1^\top P_2\bar{w}_1 + \bar{w}_2^\top P_3\bar{w}_2$ It satisfies $\alpha_{\bar{\omega}_1}|\chi_{\varepsilon_r}|^2_{\tilde{\mathcal{A}}_{\varepsilon_r}} \leq V_{\varepsilon_r}(\chi_{\varepsilon_r}) \leq \alpha_{\bar{\omega}_2}|\chi_{\varepsilon_r}|^2_{\tilde{\mathcal{A}}_{\varepsilon_r}}$ for each $\chi_{\varepsilon_r} \in \tilde{C}_{\varepsilon_r}\cup\tilde{D}_{\varepsilon_r}$ with $\alpha_1 = \min\{\lambda_{min}(P_2),\ \lambda_{min}(P_3)\}$ and $\alpha_2 = \max\{\lambda_{max}(P_2),\ \lambda_{max}(P_3)\}$. For each $\chi_{\varepsilon_r} \in \tilde{C}_{\varepsilon_r}$ $\langle\nabla V_{\varepsilon_r}(\chi_{\varepsilon_r}),\tilde{f}(\chi_{\varepsilon_r})\rangle \leq \bar{w}_1^\top(P_2A_{f_3} + A_{f_3}^\top P_2)\bar{w}_1 + \bar{w}_2^\top(P_3A_{f_4} + A_{f_4}^\top P_3)\bar{w}_2$ The conditions in (16) imply the existence of positive numbers β_1 and β_2 such that $P_2A_{f_3} + A_{f_3}^\top P_2 \leq -\beta_1 I$ $P_3A_{f_4} + A_{f_4}^\top P_3 \leq -\beta_2 I$ Then $\langle\nabla V_{\varepsilon_r}(\chi_{\varepsilon_r}),\tilde{f}_{\varepsilon_r}(\chi_{\varepsilon_r})\rangle \leq -\frac{\tilde{\beta}}{\alpha_{\bar{\omega}_2}}V_{\varepsilon_r}(\chi_{\varepsilon_r})$ where $\tilde{\beta} = \min\{\beta_1,\beta_2\} > 0$. For all $\chi_{\varepsilon_r} \in \tilde{D}_{\varepsilon_r}$ and $g \in \tilde{G}_{\varepsilon_r}(\chi_{\varepsilon_r})$, $V_{\varepsilon_r}(g) - V_{\varepsilon_r}(\chi_{\varepsilon_r}) = 0$. Now, pick a solution $\tilde{\phi}$ to $\widetilde{\mathcal{H}}_{\varepsilon_r}$ with initial condition $\tilde{\phi}(0,0) \in \tilde{C}_{\varepsilon_r}\cup\tilde{D}_{\varepsilon_r}$. Direct integration of $(t,j) \mapsto V_{\varepsilon_r}(\tilde{\phi}(t,j))$ over dom $\tilde{\phi}$ gives $V_{\varepsilon_r}(\tilde{\phi}(t,j)) \leq \exp\big(-\frac{\tilde{\beta}}{\alpha_{\bar{\omega}_2}}t\big)V_{\varepsilon_r}(\tilde{\phi}(0,0))$ for each $(t,j) \in \text{dom }\tilde{\phi}$. Now, given the relation established in (15), for any solution $\tilde{\phi}$ to $\widetilde{\mathcal{H}}_{\varepsilon_r}$, we have $jT_2 \leq t \Rightarrow -t \leq -jT_2$. Then, for any $\gamma \in (0,1)$ we have $-\gamma t \leq -\gamma T_2 j$. Moreover, $-t = -(1-\gamma)t - \gamma t \leq -(1-\gamma)t - \gamma T_2 j \leq -\min\{1-\gamma,\gamma T_2\}(t+j)$ leading to $V_{\varepsilon_r}(\tilde{\phi}(t,j)) \leq \exp\Big(-\frac{\bar{\gamma}\tilde{\beta}}{\alpha_{\bar{\omega}_2}}(t+j)\Big)V_{\varepsilon_r}(\tilde{\phi}(0,0))$ for each $(t,j) \in \text{dom }\tilde{\phi}$ where $\bar{\gamma} = \min\{1-\gamma,\gamma T_2\}$. Then, by combining this inequality with the definition of V_{ε_r}, one has $\alpha_{\bar{\omega}_1}|\chi_{\varepsilon_r}|^2_{\tilde{\mathcal{A}}_{\varepsilon_r}} \leq V_{\varepsilon_r}(\tilde{\phi}(t,j)) \leq \exp\Big(-\frac{\bar{\gamma}\tilde{\beta}}{\alpha_{\bar{\omega}_2}}(t+j)\Big)V_{\varepsilon_r}(\tilde{\phi}(0,0))$ then leveraging $V_{\varepsilon_r}(\tilde{\phi}(0,0)) \leq \alpha_{\bar{\omega}_2}|\tilde{\phi}(0,0)|^2_{\tilde{\mathcal{A}}_{\varepsilon_r}}$ we have $|\tilde{\phi}(t,j)|_{\tilde{\mathcal{A}}_{\varepsilon_r}} \leq \sqrt{\frac{\alpha_{\bar{\omega}_2}}{\alpha_{\bar{\omega}_1}}}\exp\Big(-\frac{\bar{\gamma}\tilde{\beta}}{2\alpha_{\bar{\omega}_2}}(t+j)\Big)|\tilde{\phi}(0,0)|_{\tilde{\mathcal{A}}_{\varepsilon_r}}$ Observe that this bound holds for each solution $\tilde{\phi}$ to $\widetilde{\mathcal{H}}_{\varepsilon_r}$. Maximal solutions to $\widetilde{\mathcal{H}}_{\varepsilon_r}$ are complete due to the reduction property established in Lemmas 5.4, 5.1, and 4.4. Therefore, the set $\tilde{\mathcal{A}}_{\varepsilon_r}$ is globally exponentially stable for $\widetilde{\mathcal{H}}_{\varepsilon_r}$. ■

References

[1] L. Schenato and F. Fiorentin, "Average timesynch: A consensus-based protocol for clock synchronization in wireless sensor networks," *Automatica*, vol. 47, no. 9, pp. 1878–1886, 2011.

[2] S. Graham and P. Kumar, "Time in general-purpose control systems: The control time protocol and an experimental evaluation," in *2004 43rd IEEE Conference on Decision and Control (CDC)(IEEE Cat. No. 04CH37601)*, vol. 4, pp. 4004–4009, IEEE, 2004.

[3] Y.-C. Wu, Q. Chaudhari, and E. Serpedin, "Clock synchronization of wireless sensor networks," *IEEE Signal Processing Magazine*, vol. 28, no. 1, pp. 124–138, 2010.

[4] J. R. Vig, "Introduction to quartz frequency standards," tech. rep., Army Lab Command Fort Monmouth NJ Electronics Technology and Devices Lab, 1992.

[5] N. M. Freris, S. R. Graham, and P. Kumar, "Fundamental limits on synchronizing clocks over networks," *IEEE Transactions on Automatic Control*, vol. 56, no. 6, pp. 1352–1364, 2010.

[6] D. L. Mills, "Internet time synchronization: the network time protocol," *IEEE Transactions on communications*, vol. 39, no. 10, pp. 1482–1493, 1991.

[7] J. Elson, L. Girod, and D. Estrin, "Fine-grained network time synchronization using reference broadcasts," *SIGOPS Oper. Syst. Rev.*, vol. 36, no. SI, pp. 147–163, 2002.

[8] S. Ganeriwal, R. Kumar, and M. B. Srivastava, "Timing-sync protocol for sensor networks," in *Proceedings of the 1st International Conference on Embedded Networked Sensor Systems*, SenSys '03, (New York, NY, USA), pp. 138–149, ACM, 2003.

[9] R. Olfati-Saber and R. M. Murray, "Consensus problems in networks of agents with switching topology and time-delays," *IEEE Transactions on Automatic Control*, vol. 49, pp. 1520–1533, Sept 2004.

[10] J. A. Fax and R. M. Murray, "Information flow and cooperative control of vehicle formations," *IEEE Transactions on Automatic Control*, vol. 49, pp. 1465–1476, Sep. 2004.

[11] M. Cao, A. S. Morse, and B. D. Anderson, "Reaching a consensus in a dynamically changing environment: A graphical approach," *SIAM Journal on Control and Optimization*, vol. 47, no. 2, pp. 575–600, 2008.

[12] J. He, P. Cheng, L. Shi, and J. Chen, "Time synchronization in wsns: A maximum value based consensus approach," in *2011 50th IEEE Conference on Decision and Control and European Control Conference*, pp. 7882–7887, Dec 2011.

[13] E. Garone, A. Gasparri, and F. Lamonaca, "Clock synchronization protocol for wireless sensor networks with bounded communication delays," *Automatica*, vol. 59, pp. 60–72, 2015.

[14] Y. Kikuya, S. M. Dibaji, and H. Ishii, "Fault tolerant clock synchronization over unreliable channels in wireless sensor networks," *IEEE Transactions on Control of Network Systems*, vol. 5, no. 4, pp. 1551–1562, 2017.

[15] R. Carli, A. Chiuso, L. Schenato, and S. Zampieri, "A PI consensus controller for networked clocks synchronization," *IFAC Proceedings Volumes*, vol. 41, no. 2, pp. 10289–10294, 2008.

[16] R. Carli and S. Zampieri, "Network clock synchronization based on the second-order linear consensus algorithm," *IEEE Transactions on Automatic Control*, vol. 59, pp. 409–422, Feb 2014.

[17] S. Bolognani, R. Carli, E. Lovisari, and S. Zampieri, "A randomized linear algorithm for clock synchronization in multi-agent systems," *IEEE Transactions on Automatic Control*, vol. 61, no. 7, pp. 1711–1726, 2015.

[18] S. A. Phillips, *Robust Coordination and Control of Networked Systems with Intermittent Communication*. University of California, Santa Cruz, 2018.

[19] R. Goebel, R. G. Sanfelice, and A. R. Teel, *Hybrid Dynamical Systems: Modeling, Stability, and Robustness*. Princeton University Press, 2012.

[20] M. Guarro and R. G. Sanfelice, "HyNTP: A distributed hybrid algorithm for time synchronization," 2021. https://arxiv.org/abs/2105.00165.

[21] M. Guarro and R. G. Sanfelice, "HyNTP: An adaptive hybrid network time protocol for clock synchronization in heterogeneous distributed systems," in *2020 American Control Conference (ACC)*, pp. 1025–1030, 2020.

[22] M. S. Stanković, S. S. Stanković, and K. H. Johansson, "Distributed time synchronization for networks with random delays and measurement noise," *Automatica*, vol. 93, pp. 126–137, 2018.

[23] F. Ferrante, F. Gouaisbaut, R. G. Sanfelice, and S. Tarbouriech, "State estimation of linear systems in the presence of sporadic measurements," *Automatica*, vol. 73, pp. 101 – 109, 2016.

[24] C. D. Godsil and G. F. Royle, *Algebraic Graph Theory*. 2001.

[25] B. Altin and R. Sanfelice, "Hybrid systems with delayed jumps: Asymptotic stability via robustness and lyapunov conditions," *IEEE Transactions on Automatic Control*, 08/2020 2020.

[26] K. Narendra and A. Annaswamy, "A new adaptive law for robust adaptation without persistent excitation," *IEEE Transactions on Automatic Control*, vol. 32, pp. 134–145, February 1987.

[27] K. S. Yıldırım, R. Carli, and L. Schenato, "Adaptive proportional–integral clock synchronization in wireless sensor networks," *IEEE Transactions on Control Systems Technology*, vol. 26, no. 2, pp. 610–623, 2017.

[28] C. Liao and P. Barooah, "Distributed clock skew and offset estimation from relative measurements in mobile networks with markovian switching topology," *Automatica*, vol. 49, no. 10, pp. 3015–3022, 2013.

[29] Q. M. Chaudhari, E. Serpedin, and K. Qaraqe, "On maximum likelihood estimation of clock offset and skew in networks with exponential delays," *IEEE Transactions on Signal Processing*, vol. 56, no. 4, pp. 1685–1697, 2008.

[30] Y.-P. Tian, S. Chun, G. Chen, S. Zong, Y. Huang, and B. Wang, "Delay compensation-based time synchronization under random delays: Algorithm and experiment," *IEEE Transactions on Control Systems Technology*, vol. 29, no. 1, pp. 80–95, 2020.

Marcello D. Guarro received his B.S. degree in Applied Physics in 2010, his M.S. degree in Computer Engineering in 2018, and PhD. in Computer Engineering in 2021 all from the University of California, Santa Cruz.

His research interests include modeling, observer design, stability, control, and robustness analysis of hybrid systems with applications in cyber-physical systems, clock synchronization, autonomous vehicles, and robotics.

Ricardo G. Sanfelice received the B.S. degree in Electronics Engineering from the Universidad de Mar del Plata, Buenos Aires, Argentina, in 2001, and the M.S. and Ph.D. degrees in Electrical and Computer Engineering from the University of California, Santa Barbara, CA, USA, in 2004 and 2007, respectively. In 2007 and 2008, he held postdoctoral positions at the Laboratory for Information and Decision Systems at the Massachusetts Institute of Technology and at the Centre Automatique et Systèmes at the École de Mines de Paris. In 2009, he joined the faculty of the Department of Aerospace and Mechanical Engineering at the University of Arizona, Tucson, AZ, USA, where he was an Assistant Professor. In 2014, he joined the University of California, Santa Cruz, CA, USA, where he is currently Professor in the Department of Electrical and Computer Engineering. Prof. Sanfelice is the recipient of the 2013 SIAM Control and Systems Theory Prize, the National Science Foundation CAREER award, the Air Force Young Investigator Research Award, the 2010 IEEE Control Systems Magazine Outstanding Paper Award, and the 2020 Test-of-Time Award from the Hybrid Systems: Computation and Control Conference. His research interests are in modeling, stability, robust control, observer design, and simulation of nonlinear and hybrid systems with applications to power systems, aerospace, and biology.